Estudio de las vías de supervivencia y muerte neuronal en modelos de la enfermedad de Huntington

Paola Paoletti Rubia

UNIVERSITAT DE BARCELONA

Departamento de
Biología Celular, Inmunología y Neurociencias
Facultad de Medicina

ESTUDIO DE LAS VÍAS DE SUPERVIVENCIA Y MUERTE NEURONAL EN MODELOS DE LA ENFERMEDAD DE HUNTINGTON

Tesis presentada por Paola Paoletti Rubia
para optar al título de Doctora por la Universidad de Barcelona

Programa de Doctorado en Biomedicina

III. RESULTADOS

PRIMER TRABAJO: “Dopaminergic and glutamatergic signaling crosstalk in Huntington’s disease neurodegeneration: the role of p25/Cyclin-Dependent Kinase 5”

Publicado en The Journal of Neuroscience 2008; 28(40):10090-10101

1.- Estudio de la implicación de la señalización dopaminérgica y glutamatérgica en modelos celulares *knock-in* de la enfermedad de Huntington.

1.1.- Estudiar si la expresión de la htt mutada incrementa la susceptibilidad estriatal frente a una activación dopaminérgica y si este efecto se ve modulado por la activación glutamatérgica en modelos celulares *knock-in* de la enfermedad de Huntington.

1.2.- Estudiar las vías de señalización intracelular involucradas en la mayor vulnerabilidad estriatal tras una activación dopaminérgica y glutamatérgica en modelos celulares y murinos *knock-in* de la enfermedad de Huntington, así como en muestras de pacientes afectados por la enfermeda.

En este estudio se analizó la mayor vulnerabilidad estriatal frente a la activación de los sistemas glutamatérgicos y dopaminérgicos en modelos celulares de la enfermedad de Huntington. El resultado más importante ha sido el constatar que la presencia de la htt mutada potencia la muerte celular inducida por dopamina vía la activación del receptor D_1 pero no del receptor D_2, y que esta mayor susceptibilidad se ve potenciada al activar previamente el receptor de NMDA. Dicho efecto está asociado a nivel intracelular con una aberrante activación de la vía de la quinasa Cdk5, alteración que se observa tanto en modelos murinos *knock-in* de la enfermedad de Huntington como en muestras de pacientes afectados por la enfermedad.

10090 • The Journal of Neuroscience, October 1, 2008 • 28(40):10090–10101

Neurobiology of Disease

Dopaminergic and Glutamatergic Signaling Crosstalk in Huntington's Disease Neurodegeneration: The Role of p25/Cyclin-Dependent Kinase 5

Paola Paoletti,[1,2] Ingrid Vila,[1,2] Maria Rifé,[1,2] José Miguel Lizcano,[3] Jordi Alberch,[1,2] and Silvia Ginés[1,2]

[1]Departament de Biologia Cellular, Immunologia i Neurociències, Facultat de Medicina, Institut d'Investigacions Biomèdiques August Pi i Sunyer and [2]Centro de Investigación Biomédica en Red sobre Enfermedades Neurodegenerativas, Universitat de Barcelona, E-08036 Barcelona, Spain, and [3]Institut de Neurociències i Departament de Bioquímica i Biologia Molecular, Universitat Autònoma de Barcelona, E-08193 Barcelona, Spain

Altered glutamatergic and dopaminergic signaling has been proposed as contributing to the specific striatal cell death observed in Huntington's disease (HD). However, the precise mechanisms by which mutant huntingtin sensitize striatal cells to dopamine and glutamate inputs remain unclear. Here, we demonstrate in knock-in HD striatal cells that mutant huntingtin enhances dopamine-mediated striatal cell death via dopamine D_1 receptors. Moreover, we show that NMDA receptors specifically potentiate the vulnerability of mutant huntingtin striatal cells to dopamine toxicity as pretreatment with NMDA increased D_1R-induced cell death in mutant but not wild-type cells. As potential underlying mechanism of increased striatal vulnerability, we identified aberrant cyclin-dependent kinase 5 (Cdk5) activation. We demonstrate that enhanced Cdk5 phosphorylation and increased calpain-mediated conversion of the Cdk5 activator p35 into p25 may account for the deregulation of Cdk5 associated to dopamine and glutamate receptor activation in knock-in HD striatal cells. Moreover, supporting a detrimental role of Cdk5 in striatal cell death, neuronal loss can be widely prevented by roscovitine, a potent Cdk5 inhibitor. Significantly, reduced Cdk5 expression together with enhanced Cdk5 phosphorylation and p25 accumulation also occurs in the striatum of mutant *Hdh*^{Q111} mice and HD human brain suggesting the relevance of deregulated Cdk5 pathway in HD pathology. These findings provide new insights into the molecular mechanisms underlying the selective vulnerability of striatal cells in HD and identify p25/Cdk5 as an important mediator of dopamine and glutamate neurotoxicity associated to HD.

Key words: striatum; neurotoxicity; huntingtin; dopamine D_1 receptors; glutamate; p25

Introduction

Huntington's disease (HD) is a progressive neurological disorder characterized by chorea, cognitive decline, and psychiatric disturbances (MacDonald et al., 2003; Pérez-Navarro et al., 2006). Dysfunction and death of striatal medium-spiny neurons is the major feature of neuropathological changes in HD (Martin and Gusella, 1986; de la Monte et al., 1988). Although it is not known why spiny neurons are preferentially targeted for degeneration, there is evidence to support the idea that mutant huntingtin toxicity may involve excitotoxicity caused by aberrant NMDA receptor activation (Pérez-Navarro et al., 2006; Fan and Raymond, 2007). In addition to glutamatergic afferents, the striatum also receives the densest dopaminergic innervation in the brain from the ventral midbrain neurons. Despite the high concentration of dopamine (DA) in the striatum, a number of studies have revealed a potential toxic role of DA in the nervous system (Jakel and Maragos, 2000). Thus, exposure of primary striatal neurons to DA causes significant neurotoxicity with increased free radical production and accelerated neuronal death (Wersinger et al., 2004). Moreover, there is increasing evidence that the dopaminergic system may contribute to HD neuropathology. Data from striatal primary neurons that express exon-1 mutant huntingtin indicates that DA exacerbates mutant huntingtin toxicity via reactive oxygen species production and D_2 receptor activation (Charvin et al., 2005; Benchoua et al., 2008). Furthermore, in double mutant mice expressing endogenous levels of exon-1 mutant huntingtin and knock-out for the dopamine transporter, DA accelerates protein aggregation and motor dysfunction (Cyr et al., 2006). These data suggest that disturbed DA and NMDA signaling may participate in the enhanced sensitivity of striatal neurons to huntingtin toxicity. In this line, Tang et al. (2007) have reported that dopamine potentiates glutamate-induced apoptosis in cultured striatal neurons from *YAC128* HD mice via activation of D_1 receptors. However, little is known about the molecular mechanisms that underlie the increased vulnerability of mutant huntingtin striatal cells to dopamine and glutamate inputs.

Cyclin-dependent kinase 5 (Cdk5) is a serine/threonine ki-

Received July 10, 2008; accepted Aug. 18, 2008.

This work was supported by grants from Ministerio de Educación y Ciencia, Centro de Investigaciones Biomédicas en Red sobre Enfermedades Neurodegenerativas, Fundació La Marató de TV3, and HighQ Foundation. P.P. and M.R. are fellows of the HighQ Foundation. We thank Dr. M. Macdonald for the knock-in striatal cell lines and knock-in HD mice and Dr. P Davis for tau antibodies. We are very grateful to Cristina Herranz, Ana Lopez, and M. Teresa Muñoz for technical assistance. We thank Banc de Teixits Neurològics (University of Barcelona, Barcelona, Spain) for human tissue samples. We thank C. A. Saura and members of our laboratory for helpful discussion.

Correspondence should be addressed to Silvia Ginés, Universitat de Barcelona, Casanova 143, E-08036 Barcelona, Spain. E-mail: silviagines@ub.edu.

DOI:10.1523/JNEUROSCI.3237-08.2008

 0270-6474/08/2810090-12$15.00/0

nase whose activity is primarily restricted to the nervous system where its main activator p35 is expressed. Although Cdk5 is essential for brain development, many neurodegenerative diseases involve sustained activation of Cdk5 in neurons (Cruz and Tsai, 2004; Dhariwala and Rajadhyaksha, 2008). Several studies indicate that Cdk5 becomes a cell death inductor when it binds to p25, the calpain-mediated cleaved product of p35 (Lee et al., 2000). Thus, accumulation of p25 has been observed in neurons treated with glutamate or oxidative stress as well as in animal models of several neurodegenerative diseases (Cruz and Tsai, 2004; Dhariwala and Rajadhyaksha, 2008). Notably, treatment with 3-nitropropionic, the systemic administration of which produces selective striatal degeneration with symptoms resembling those of HD (Beal et al., 1993), induces striatal but not cortical Cdk5 activation (Crespo-Biel et al., 2007; Akashiba et al., 2008). More recently, it has been postulated for Cdk5 a role in dopaminergic neurodegeneration. Thus, 1-methyl-4-phenyl-1,2,3,6-tetrahydropyridine (MPTP)-induced dopaminergic cell loss involves enhanced Cdk5 activity and increased conversion of p35 to the pathogenic p25 form (Smith et al., 2003, 2006).

The above observations prompted us to explore the involvement of aberrant glutamatergic and dopaminergic signaling in striatal neurodegeneration in HD to determine whether Cdk5 might account for this neurotoxic effect. Our data suggest that mutant huntingtin alters NMDAR and D_1R signaling via Cdk5 to increase the vulnerability of striatal cells to neurotoxicity.

Materials and Methods

Reagents and antibodies. NMDA, (±)-SKF-38393 hydrochloride, (±)-Quinpirole dihydrochloride, R(+)-SCH-23390 hydrochloride, (-)-MK-801 hydrogen maleate, EGTA, roscovitine, and SP600125 were obtained from Sigma-Aldrich. Hoechst 33258 pentahydrate was from Invitrogen. Anti-p35 (C-19), anti-phospho-Cdk5 (Tyr^{15}), and anti-Cdk5 (J-3) antibodies were purchased from Santa Cruz Biotechnology. Anti-phospho-stress-activated protein kinase (SAPK)/c-Jun N-terminal protein kinase (JNK) (Thr^{183}/Tyr^{185}) and anti-SAPK/JNK were from Cell Signaling Technologies. Paired helical filament (PHF)-1 and TG5 anti-tau antibodies were a generous gift from Peter Davis (Albert Einstein College of Medicine, Bronx, NY). Anti-green fluorescent protein (GFP) was obtained from Clontech. Anti-α-spectrin was purchased from Millipore. Anti-α-tubulin was from Sigma-Aldrich.

Cell cultures. Conditionally immortalized wild-type $STHdh^{Q7}$ and mutant $STHdh^{Q111}$ striatal neuronal progenitor cell lines expressing endogenous levels of normal and mutant huntingtin with 7 and 111 glutamines, respectively, have been described previously (Trettel et al., 2000). Striatal cells were grown at 33°C in DMEM (Sigma-Aldrich), supplemented with 10% fetal bovine serum (FBS), 1% streptomycin-penicillin, 2 mM L-glutamine, 1 mM sodium pyruvate, and 400 μg/ml G418 (Geneticin; Invitrogen).

Genetic Huntington's disease mouse model and postmortem brain tissues. Hdh^{Q111} knock-in mice expressing mutant huntingtin with 111 glutamine residues have been described previously (Wheeler et al., 1999). Animals were deeply anesthetized with CO_2 and decapitated. Striatum was dissected from 9-month-old homozygous mutant $Hdh^{Q111/Q111}$ and wild-type $Hdh^{Q7/Q7}$ littermate offspring, obtained from the mating of male and female $Hdh^{Q111/Q7}$ heterozygotes. The animals were housed under a 12 h light/dark cycle with food and water *ad libitum*. All procedures were performed in accordance with the National Institutes of Health and were approved by the local animal care committee of the Universitat de Barcelona (99/01) and the Generalitat de Catalunya (00/1094).

Samples of the caudate and putamen nucleus from three patients with HD (with death at end-stage disease at 71, 68, and 65 years, postmortem intervals of 4–15 h) and three control cases (42, 77, and 74 years, postmortem intervals of 4–23 h) were supplied by the Banc de Teixits Neurològics (Servei Científico-Tècnic, Universitat de Barcelona, Barcelona, Spain). All of the ethical guidelines contained within the latest Declaration of Helsinki were taken into consideration, and informed consent was obtained from all subjects under study.

Drug treatments of striatal cell lines. To induce NMDA excitotoxicity, wild-type $STHdh^{Q7}$ and mutant knock-in $STHdh^{Q111}$ striatal cells were exposed to 500 or 50 μM NMDA in Locke's solution (154 mM NaCl, 5.6 mM KCl, 2.3 mM $CaCl_2$, 3.6 mM $NaHCO_3$, 5 mM HEPES, 5.6 mM glucose, and 10 μM glycine) for 30 min. After treatment, the medium was replaced by fresh DMEM medium with 2.5% FBS.

To assess the effect of dopamine receptor activation, wild-type $STHdh^{Q7}$ and mutant $STHdh^{Q111}$ striatal cells were treated for 24 h in DMEM medium (2.5% FBS) with different concentrations of the D_1 receptor agonist SKF38393 (30, 60, 80, or 100 μM) or the D_2 receptor agonist quinpirole (30, 60, or 150 μM).

In some experiments, cultures were treated with the D_1 receptor antagonist (SCH-23390, 10 μM), the JNK inhibitor (SP600125, 10 μM), or the Cdk5 inhibitor (roscovitine, 20 μM) 1 h before NMDA or SKF38393 treatments.

To study Cdk5 and p35/p25 protein levels, wild-type STHdhQ7 and mutant knock-in STHdhQ111 striatal cells were first placed in DMEM serum-free medium for 3 h. For the NMDA treatment, cells were exposed to 500 μM NMDA in Locke's solution for 30 min. After treatment, the medium was replaced by fresh DMEM serum-free medium, and total cell extracts were obtained at different time periods (5, 15, 30, and 60 min). For the SKF38393 treatment, cells were exposed to Locke's solution for 30 min before the addition of SKF38393 (100 μM) in fresh DMEM serum-free medium. Total extracts were obtained at different time periods (5, 15, 30, and 60 min) after SKF38393 treatment. Finally, to assess the combined treatment, cells were pre-exposed to 500 μM NMDA in Locke's solution for 30 min. After treatment, the medium was replaced by fresh DMEM serum-free medium containing 100 μM SKF38393 and total cell extracts were obtained at different time periods (5, 15, 30, and 60 min) after SKF38393 treatment.

To test the role of calcium influx in the p35/p25 protein levels, mutant STHdhQ111 striatal cells were first placed in DMEM serum-free medium for 3 h and then exposed to 25 μM MK-801 or 400 μM EGTA in DMEM serum-free medium for 6 h. Total cell extracts were obtained after treatment.

Cell survival. Cell survival was assessed by nuclear DNA staining with Hoechst 33258. Cells were washed twice with PBS, fixed with 4% paraformaldehyde in PBS for 10 min, washed twice in PBS, and stained with Hoechst 33258 (1 μg/ml) for 5 min. Stained cells were then washed twice with PBS and mounted under glass coverslips with Mowiol. Cell survival is represented as the proportion of Hoechst-stained nuclei counted in treated cells compared with the number of control (vehicle-treated) cells (100%). Forty fields were counted per condition and experiment, comprising at least 30–40 cells. Data are given as mean ± SD of values obtained in three independent experiments performed in triplicate.

Cell transfection. For the study of polyQ length-dependent Cdk5 and p-Cdk5 expression, wild-type $STHdh^{Q7}$ striatal cells were transfected using Lipofectamine 2000 as described by the manufacturer (Invitrogen). Wild-type $STHdh^{Q7}$ at 50% confluence were transfected with three different constructs containing the mutant exon 1 of the huntingtin gene with different CAG/CAA repeats and with enhanced GFP: 23, Q23htt; 72, Q72htt and 103, Q103htt (Kazantsev et al., 1999) (generously provided by Dr. George M. Lawless, Cure HD Initiative, Reagent Resource Bank of the Hereditary Disease Foundation, New York, NY). The protein extracts were prepared 24 h after transfection.

Western blot analysis. Total cellular extracts were collected in lysis buffer containing 50 mM Tris base, pH 7.4, 150 mM NaCl, 2 mM EDTA, 0.1 mM phenylmethylsulphonyl fluoride, 1% NP-40, and supplemented with 1 mM sodium orthovanadate and protease inhibitor mixture (Sigma-Aldrich). Samples were centrifuged at 10,000 × *g* for 10 min and the protein contents determined by (detergent-compatible) protein assay (Bio-Rad). Protein extracts (20–40 μg) were mixed with 5× SDS sample buffer, boiled for 5 min, resolved by 8–10% SDS-PAGE, and transferred to nitrocellulose membranes (Whatman Schleicher and Schuell). Blots were blocked in 10% nonfat powdered milk in TBS-T (50 mM Tris-HCl, 150 mM NaCl, pH 7.4, 0.05% Tween 20) for 30 min at

room temperature. The membranes were then incubated overnight at 4°C with primary antibodies [phospho-JNK (Thr^{183}/Tyr^{185}) (1:1000), total JNK (1:1000), p35 (1:1000), phospho-Cdk5 (Tyr^{15}) (1:5000), total Cdk5 (1:1000), GFP (1:500), α-spectrin (1:1000), TauG5 (1:500), PHF-1 (1:500), or α-tubulin (1:50,000)]. The membranes were then rinsed three times with Tris-buffered saline–Tween 20 (TBS-T) and incubated with horseradish peroxidase-conjugated secondary antibody for 1 h at room temperature. After washing for 30 min with TBS-T, the membranes were developed using the enhanced chemiluminescence substrate kit (Santa Cruz Biotechnology). The Gel-Pro densitometry program (Gel-Pro Analyzer for Windows, version 4.0.00.001) was used to quantify the different immunoreactive bands relative to the intensity of the α-tubulin band in the same membranes. We ensured signals were within a linear range of detection for the ECL reagent on Hyperfilm ECL (GE Healthcare) by probing increasing amounts of lysate with the relevant antibody. Data are expressed as the mean ± SD of band density obtained in three independent experiments.

Cdk5 kinase activity. Cdk5 was immunoprecipitated with 1 μg of anti-Cdk5 agarose conjugated antibody (C-8; Santa Cruz Biotechnology) from 500 μg of total cell lysates obtained from wild-type STHdh^{Q7} and mutant STHdh^{Q111} striatal cells treated with 100 μM SKF38393 alone or pre-exposed (30 min) to NMDA before SKF38393 treatment. The immunoprecipitates were washed three times with lysis buffer and twice with kinase buffer (50 mM Tris, pH 7.5, 0.1% β-mercaptoethanol, 0.1 mM EGTA, 0.1 mM EDTA). The standard assay contained the following (50 μl total volume): washed agarose immunoprecipitate, 50 mM Trs-HCl, pH 7.5, 0.1 mM EGTA, 0.1% β-mercaptoethanol, 10 mM magnesium acetate, 0.1 mM [γ-^{32}P]-ATP (5 μCi), and 200 μM of substrate (peptide histone 1; Jena Bioscience). The assays were performed for 60 min at 30°C, and the assay tubes were agitated continuously to keep the immunoprecipitate in suspension. Incorporation of [γ-^{32}P]-phosphate into peptide substrate was determined using p81 phosphocellulose paper. Papers were washed in 0.5% ortophosphoric acid, dried, and Cherenkov radiation was counted. Control experiments were performed in parallel without the peptide substrate.

Statistical analysis. All of the data were analyzed with the program Graph Pad Prism version 4.0 (GraphPad Software). Results are expressed as mean ± SD. Experimental data were analyzed either by a one- or two-way ANOVA followed by the *post hoc* Bonferroni's multiple comparison test or by Student's *t* test. A value of $p < 0.05$ was accepted as denoting statistical significance.

Results

D_1 receptor activation increases neuronal death in STHdh^{Q111} striatal cells

To determine whether mutant huntingtin enhances the vulnerability of striatal cells to dopamine, immortalized striatal cells expressing endogenous levels of full-length wild-type STHdh^{Q7} or mutant STHdh^{Q111} huntingtin were treated with increasing concentrations of the D_1 receptor agonist SKF38393 (0–100 μM) or the D_2 receptor agonist quinpirole (0–150 μM) followed by the determination of cell survival. SKF38393 treatment caused a dose-dependent increase in neuronal cell death in both wild-type and mutant striatal cells (Fig. 1*A*). Two-way ANOVA analysis for drug treatment and genotype showed that the effect was statistically significant ($F_{(4,15)} = 444.30$, $p < 0.001$; $F_{(1,15)} = 192.04$, $p \leq 0.001$, respectively). Importantly, the interaction between genotype and treatment was also statistically significant ($F_{(4,15)} = 31.69$; $p < 0.001$), indicating that the two cell genotypes responded differently to the SKF38393 treatment. Thus, at all SKF38393 concentrations tested, the reduction in cell survival was significantly higher in mutant STHdh^{Q111} than it was in wild-type STHdh^{Q7} cells, with a maximal difference detected at 100 μM SKF38393 (wild type, 64 ± 11% vs mutant, 39 ± 6%; $p \leq 0.001$). It should be noted that (1) at the lower tested concentration (SKF38393 30 μM) only mutant huntingtin STHdh^{Q111} cells exhibited a reduction in cell survival (~20%; $p \leq 0.001$), and (2) the decrease in cell survival in STHdh^{Q7} wild-type cells reached a maximum at 80 μM SKF38393 (64 ± 11%; $p \leq 0.001$), whereas STHdh^{Q111} mutant cells still exhibited higher cell death at 100 μM SKF38393 (~8% more compared with 80 μM SKF38393; $p \leq 0.05$). Importantly, coincubation with the D_1-selective antagonist SCH23390 significantly reduced SKF38393-induced cell death near to that of control levels in both wild-type and mutant huntingtin cells (~85 ± 10% and 79 ± 11%; $p \leq 0.001$, respectively) (Fig. 1*B*). No effect on neuronal survival was observed after stimulation of D_2 receptors with quinpirole (Fig. 1*A*). Thus, our results imply that D_1 receptor activation mediates the dopaminergic toxic effect observed in wild-type and mutant knock-in striatal cells and that full-length mutant huntingtin expression potentiates dopamine-cell death through D_1 but not D_2 receptors.

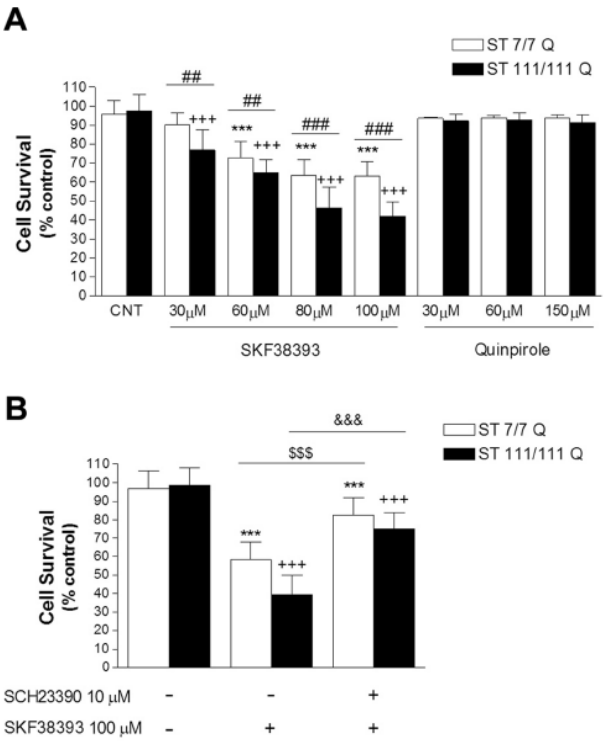

Figure 1. Increased dopamine D_1-receptor-mediated cell death in STHdh^{Q111} striatal cells. ***A***, Wild-type (ST7/7Q) and mutant (ST1111/111Q) striatal cells were treated with different concentrations of the D_1 receptor agonist SKF38393 (30, 60, 80, or 100 μM) or the D_2 receptor agonist quinpirole (30, 60, or 150 μM) during 24 h. After treatment, cell survival was measured by scoring the percentage of Hoechst-stained nuclei. Forty fields were counted per condition per experiment, comprising at least 30–40 cells. Results are expressed as percentage of control (vehicle-treated) cells, and data are the mean ± SD of three independent experiments performed in triplicate. A full statistical analysis by the two-way ANOVA is described in the text. $^{***}p < 0.001$ treated versus vehicle-treated wild-type cells; $^{+++}p < 0.001$ treated versus vehicle-treated mutant cells; $^{\#\#}p < 0.01$, $^{\#\#\#}p < 0.001$ treated mutant cells versus treated wild-type cells (Bonferroni's multiple comparison test). CNT, Control. ***B***, Wild-type and mutant striatal cells were treated (1 h) with the D_1 receptor antagonist SCH23390 (10 μM) before SKF38393 treatment (100 μM). Cell survival was assessed 24 h later by scoring the percentage of Hoechst-stained nuclei. Forty fields were counted per condition per experiment, comprising at least 30–40 cells. Results are expressed as percentage of control (vehicle-treated) cells, and data are the mean ± SD of three independent experiments performed in triplicate. $^{***}p < 0.001$ treated versus vehicle-treated wild-type cells; $^{+++}p < 0.001$ treated versus vehicle-treated mutant cells; $^{\$\$\$}p < 0.001$ SCH23390 plus SKF38393-treated wild-type cells versus SKF38393-treated wild-type cells; $^{\&\&\&}p < 0.001$ SCH23390 plus SKF38393-treated mutant cells versus SKF38393-treated mutant cells as determined by one-way ANOVA followed by Bonferroni's multiple comparison test.

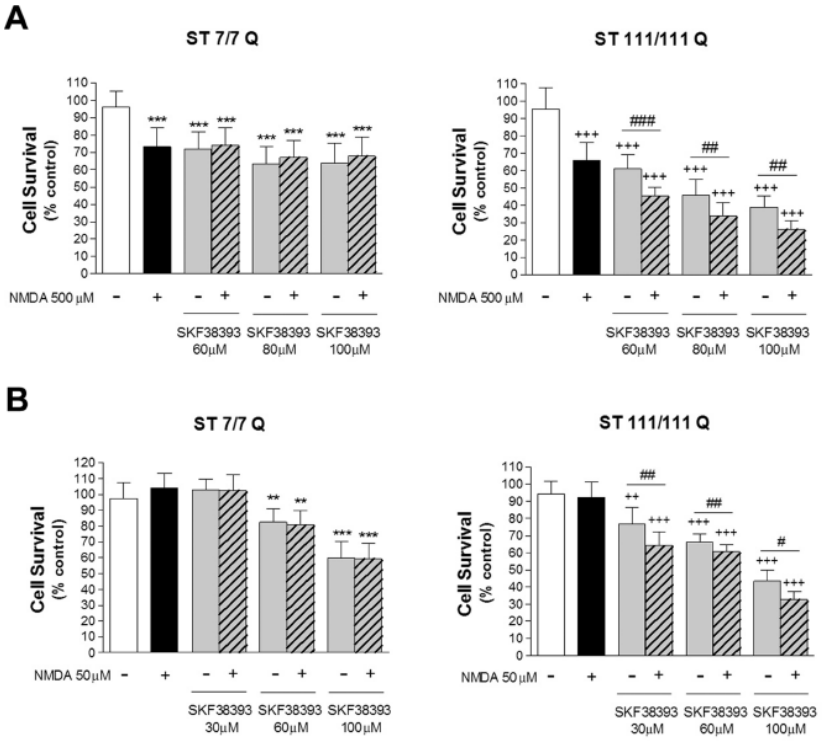

Figure 2. NMDA potentiates the toxic effect of D_1-receptor activation in STHdh^{Q111} striatal cells. ***A***, Wild-type (ST7/7Q) and mutant (ST111/111Q) striatal cells were treated with a toxic concentration of NMDA (500 μM) for 30 min before treatment with different concentrations of SKF38393 (60, 80, or 100 μM). Cell survival was assessed 24 h later by scoring the percentage of Hoechst-stained nuclei. ***B***, Wild-type and mutant striatal cells were exposed to a subtoxic concentration of NMDA (50 μM) for 30 min before treatment with different concentrations of SKF38393 (30, 60, or 100 μM). Cell survival was measured 24 h later by scoring the percentage of Hoechst-stained nuclei. Forty fields were counted per condition per experiment, comprising at least 30–40 cells. Results are expressed as percentage of control (vehicle-treated) cells, and data are the mean ± SD of three independent experiments performed in triplicate. A full statistical analysis by the two-way ANOVA is described in the text. $^{**}p < 0.01$, $^{***}p < 0.001$ treated versus vehicle-treated wild-type cells; $^{++}p < 0.01$, $^{+++}p < 0.001$ treated versus vehicle-treated mutant cells; $^{\#}p < 0.05$, $^{\#\#}p < 0.01$, $^{\#\#\#}p < 0.001$ NMDA plus SKF38393-treated mutant cells versus SKF38393-treated mutant cells (Bonferroni's multiple comparison test).

NMDA enhances dopamine D_1 receptor-mediated cell death selectively in STHdh^{Q111} cells

Previous results from our laboratory have demonstrated that mutant STHdh^{Q111} striatal cells display enhanced sensitivity to NMDA receptor activation (Xifró et al., 2008). Therefore, we next analyzed whether NMDA treatment potentiates the neurotoxic effect of dopamine. We first analyzed the role of a toxic concentration of NMDA (500 μM) on cell death induced by D_1R activation. Wild-type STHdh^{Q7} and mutant STHdh^{Q111} striatal cells were exposed for 30 min to NMDA before SKF38393 treatment, and cell survival was analyzed 24 h later. Pretreatment with NMDA failed to increase SKF38393-induced cell death in wild-type STHdh^{Q7} cells (Fig. 2*A*). Two-way ANOVA for SKF38393 treatment and wild-type group (control and pretreated with NMDA) showed that the effect was statistically significant for drug treatment ($F_{(3,12)} = 285.6$; $p \leq 0.001$) but not for wild-type group ($F_{(1,12)} = 0.97$; $p = 0.33$). Two-way ANOVA analysis also revealed lack of interaction between factors ($F_{(3,12)} = 0.38$; $p = 0.77$). In contrast, mutant STHdh^{Q111} striatal cells exhibited a significant decrease in cell survival rates when pre-exposed to NMDA compared with SKF38393 treatment alone (Fig. 2*A*). Statistical analysis revealed a main effect of NMDA pretreatment in SKF38393-induced cell death in mutant huntingtin striatal cells [$F_{(3,12)} = 740.23$, $p < 0.001$ for SKF38393 treatment; $F_{(1,12)} = 97.07$, $p \leq 0.001$ for mutant group (control and pretreated with NMDA)]. Notably, two-way ANOVA analysis also revealed a statistically significant mutant group × SKF38393 treatment interaction ($F_{(3,12)} = 13.4$; $p \leq 0.001$), indicating that mutant huntingtin cells responded differently to SKF38393 treatment when pre-exposed to NMDA toxic concentrations (Fig. 2*A*). It is important to remark that this effect was observed at concentrations of both SKF38393 and NMDA that induced moderate cell death.

To analyze further the effect of NMDA and SKF38393 on striatal cell death, we next evaluated whether a subtoxic concentration of NMDA (50 μM) modulates D_1R-mediated cell death. Consistent with the lack of an additive effect at toxic NMDA concentrations, wild-type STHdh^{Q7} striatal cells pretreated with 50 μM NMDA did not show increased cell death to that reported for SKF38393 treatment alone (Fig. 2*B*). Two-way ANOVA for SKF38393 treatment and wild-type group (control and pretreated with NMDA) showed that the effect was statistically significant for drug treatment ($F_{(3,12)} = 814.7$; $p \leq 0.001$) but not for wild-type group ($F_{(1,12)} = 0.92$; $p = 0.35$). No interaction between factors was demonstrated by two-way ANOVA analysis ($F_{(3,12)} = 0.30$; $p = 0.82$). Interestingly, NMDA preexposure was still found to potentiate the cell death induced by SKF38393 treatment in mutant STHdh^{Q111} striatal cells [$F_{(1,12)} = 481.68$, $p < 0.001$ for SKF38393 treatment; $F_{(1,12)} = 49.6$, $p \leq 0.001$ for mutant group (control and pretreated with NMDA)]. Moreover, two-way ANOVA analysis showed that the interaction between factors was statistically significant ($F_{(3,12)} = 9.07$; $p \leq 0.001$), which indicates that the curve of dose-dependent cell death induced by SKF38393 was different in mutant cells when pre-exposed to subtoxic NMDA concentrations. Together, these data indicate that NMDA enhances the sensibility of mutant but not wild-type striatal cells to D_1 receptor activation.

JNK activation is not associated with NMDA and SKF38393-mediated neurotoxicity in STHdh^{Q111} cells

Activation of the JNK may contribute to neuronal cell death after excitotoxicity (Brecht et al., 2005; Centeno et al., 2007). To investigate the potential role of the JNK pathway in the neurotoxic effect of NMDA and SKF38393, wild-type STHdh^{Q7} and mutant STHdh^{Q111} striatal cells were treated with 500 μM NMDA or 100 μM SKF38393, and the levels of total and phospho-JNK were determined by Western blot analysis. The immunoblot results revealed that neither NMDA nor SKF38393 exposure induced phosphoactivation of JNK (Fig. 3*A*). Moreover, analysis of wild-type and mutant cells exposed to 500 μM NMDA for 30 min before SKF38393 treatment revealed that a combination of both drugs did not increase JNK phosphorylation either (Fig. 3*A*). In

line with the lack of phospho-JNK activation, pre-exposure of wild-type STHdh^{Q7} and mutant STHdh^{Q111} huntingtin cells to 10 μM SP600125, a JNK inhibitor, did not rescue wild-type or mutant cells from neurotoxic cell death mediated by NMDA or SKF38393 or both (Fig. 3*B*). These results indicate that JNK does not participate in the observed neurotoxicity induced by NMDA or D_1R activation in STHdh^{Q7} and STHdh^{Q111} cells.

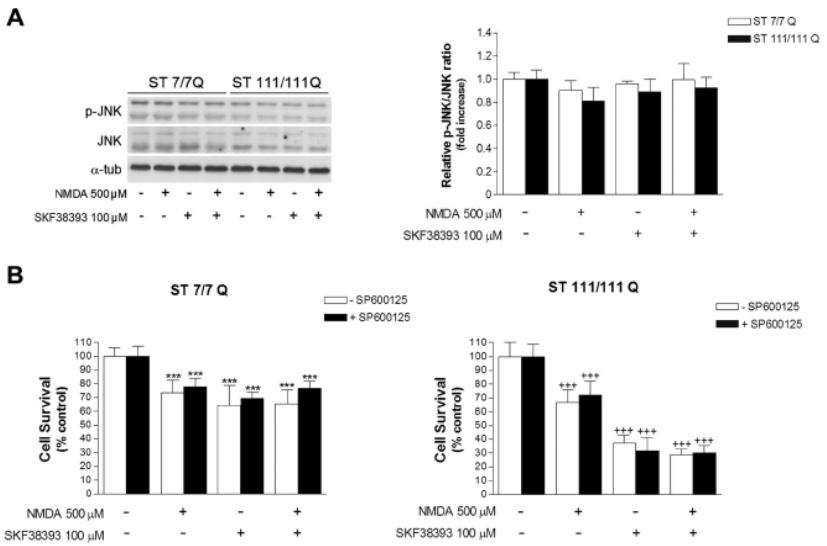

Figure 3. JNK activation is not associated with NMDA and dopamine-mediated neurotoxicity in wild-type STHdh^{Q7} and mutant STHdh^{Q111} striatal cells. ***A***, Representative Western blot showing levels of p-JNK, JNK, and α-tubulin as a loading control, from wild-type (ST7/7Q) and mutant (ST111/111Q) striatal cells treated with NMDA (500 μM) or SKF38393 (100 μM) alone, or preincubated with NMDA (30 min) before SKF38393 treatment. Total cell extracts were obtained 30 min after treatment. The histogram represents the relative p-JNK/JNK ratio expressed as fold increase versus control cells. Values are given as mean ± SD of three independent experiments. ***B***, Wild-type (ST7/7Q) and mutant (ST111/111Q) striatal cells pretreated (1 h) with the JNK inhibitor SP600125 (10 μM) were exposed to NMDA (500 μM) or SKF38393 (100 μM) alone, or preincubated with NMDA before SKF38393 exposure. Cell survival was evaluated 24 h later by scoring the percentage of Hoechst-stained nuclei. Forty fields were counted per condition per experiment, comprising at least 30–40 cells. Results are expressed as percentage of control (vehicle-treated) cells, and data are the mean ± SD of three independent experiments performed in triplicate. $^{***}p < 0.001$ treated versus vehicle-treated wild-type cells; $^{+++}p < 0.001$ treated versus vehicle-treated mutant cells as determined by one-way ANOVA followed by Bonferroni's multiple comparison test.

NMDA potentiates D_1R-induced phosphorylation of Cdk5 in mutant STHdh^{Q111} cells

Deregulation of Cdk5 activity has been associated to neuronal cell death in several neurodegenerative disorders (Cruz and Tsai, 2004). To determine whether Cdk5 activation was involved in the increased vulnerability of mutant STHdh^{Q111} cells to NMDAR and D_1R activation, we first analyzed the levels of total and phosphorylated Cdk5 (Tyr 15) in extracts obtained from wild-type STHdh^{Q7} and mutant STHdh^{Q111} striatal cells (Fig. 4*A*). Immunoblot analysis revealed that total Cdk5 levels were lower in mutant cells than they were in wild-type cells (~2-fold; $p \leq 0.001$), whereas the levels of p-Tyr^{15} Cdk5 were slightly increased (~1.2-fold; $p \leq 0.05$). Therefore, a significant ~3-fold increase in the p-Tyr^{15} Cdk5/Cdk5 ratio ($p \leq 0.001$) was apparent in mutant cells compared with wild-type cells.

To determine whether deregulation of Cdk5 pathway was dependent on mutant huntingtin expression, wild-type striatal cells were transfected with different constructs encoding for green fluorescent protein-tagged exon-1 mutant huntingtin protein with 23, 72, or 103 CAG repeats (Q23, Q72, and Q103), and total extracts were analyzed by Western blot. The results, shown in Figure 4*B*, revealed an inverse relationship between changes in Cdk5 and the length of the CAG repeat. Thus, reduced Cdk5 expression along with higher Tyr^{15}-Cdk5 phosphorylation was found in wild-type striatal cells transfected with 72 or 103 poly-Q containing exon-1 mutant huntingtin compared with those transfected with the normal poly-Q length (Q23). These data suggest that changes on Cdk5 pathway are directly dependent on mutant huntingtin expression.

We next analyzed whether activation of NMDA and D_1 receptors was associated with changes in Cdk5 expression and phosphorylation. Exposure of wild-type STHdh^{Q7} and mutant STHdh^{Q111} striatal cells to NMDA resulted in a similar time-dependent increase in Cdk5 phosphorylation. Statistical analysis using two-way ANOVA revealed a significant time interval effect ($F_{(4,25)} = 16.03$; $p < 0.001$) without differences between genotypes ($F_{(1,25)} = 3.57$; $p = 0.08$) (Fig. 4*C*). The analysis also demonstrated no interaction between factors ($F_{(4,25)} = 0.57$; $p = 0.7$). Thus, the increase in Cdk5 phosphorylation was already evident at 5 min, maximal at 15 min, and remained high even 60 min after treatment. In contrast, in the presence of 100 μM SKF38393, the kinetic of Cdk5 phosphorylation differed in mutant STHdh^{Q111} and wild-type STHdh^{Q7} cells (Fig. 4*D*). Statistical analysis using two-way ANOVA revealed a significant effect of genotype ($F_{(1,25)} = 39.36$; $p < 0.001$) and time ($F_{(4,25)} = 11.85$; $p < 0.001$) and a significant genotype × treatment interaction ($F_{(4,25)} = 20.16$; $p < 0.001$), which demonstrates that the time-dependent phosphorylation of Cdk5 induced by SKF38393 differs between wild-type and mutant huntingtin striatal cells. Thus, wild-type STHdh^{Q7} cells and mutant STHdh^{Q111} cells showed a significant increase in Cdk5 phosphorylation induced by SKF38393 at 5 min (~8-fold; $p \leq 0.001$). However, at longer periods, no higher increase in p-Cdk5 was observed in wild-type STHdh^{Q7} cells, whereas mutant STHdh^{Q111} cells exhibited a sustained increase in Cdk5 phosphorylation that was maximal at 60 min after treatment (~17-fold; $p \leq 0.001$) (Fig. 4*D*). These data suggest a dual role of mutant huntingtin on the Cdk5 pathway by reducing the total expression of Cdk5 and enhancing D_1R-mediated Cdk5 phosphorylation.

Finally, we investigated whether pretreatment with NMDA modified the D_1R-mediated phosphorylation of Cdk5 in wild-type STHdh^{Q7} and mutant STHdh^{Q111} striatal cells. Exposure of wild-type STHdh^{Q7} cells to NMDA before SKF38393 treatment did not change the pattern of Cdk5 phosphorylation compared with SKF38393 alone ($F_{(1,25)} = 0.89$; $p = 0.35$) (Fig. 4*E*). However, mutant STHdh^{Q111} cells pre-exposed to NMDA exhibited higher Cdk5 phosphorylation compared with those treated with SKF38393 alone ($F_{(1,25)} = 147.07$; $p < 0.001$) without significant interaction between treatment and time ($F_{(4,25)} = 2.21$; $p = 0.092$). These results demonstrate that in the presence of mutant huntingtin, activation of Cdk5 by D_1R is potentiated by NMDAR activation.

STHdh^{Q111} mutant cells exhibited higher p25 levels

Conversion of p35 into p25 by Ca^{2+}-dependent calpain activation has been suggested to deregulate Cdk5 activity in several

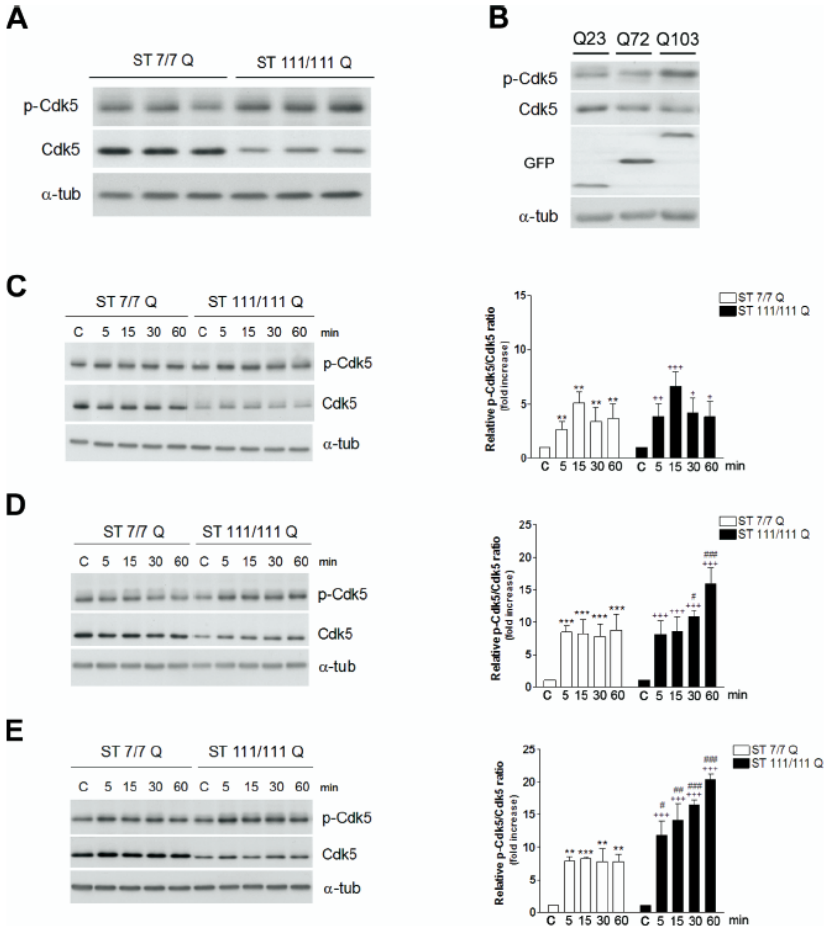

Figure 4. NMDA receptor activation potentiates D_1R-induced Cdk5 phosphorylation in mutant STHdh^{Q111} cells. *A*, Representative Western blot showing levels of p-Cdk5, Cdk5, and α-tubulin as a loading control from wild-type (ST7/7Q) and mutant (ST111/111Q) striatal cells. *B*, Representative Western blot showing levels of p-Cdk5, Cdk5, and GFP and α-tubulin as a loading control from wild-type striatal cells transfected with different constructs encoding for enhanced fluorescent protein-tagged exon-1 mutant huntingtin protein with 23 (Q23), 72 (Q72), or 103 (Q103) CAG repeats. *C–E*, Representative Western blot showing levels of p-Cdk5, Cdk5, and α-tubulin as a loading control from wild-type (ST7/7Q) and mutant (ST111/111Q) cell extracts obtained after treatment with NMDA 500 μM (*C*), SKF38393 100 μM (*D*), or a pretreatment with NMDA before SKF38393 exposure (*E*). Total cell extracts were obtained at different time periods (5, 15, 30, and 60 min) after treatment. The histograms represent the relative p-Cdk5/Cdk5 ratio expressed as fold increase versus control (vehicle-treated) cells. Values are given as mean ± SD of five independent experiments. A full statistical analysis by the two-way ANOVA is described in the text. $^{**}p < 0.01$, $^{***}p < 0.001$ treated versus vehicle-treated wild-type cells; $^{+}p < 0.05$, $^{++}p < 0.01$, $^{+++}p < 0.001$ treated versus vehicle-treated mutant cells; $^{\#}p < 0.05$, $^{\#\#}p < 0.01$, $^{\#\#\#}p < 0.001$ treated mutant cells versus treated wild-type cells (Bonferroni's multiple comparison test).

neurodegenerative disorders (Dhariwala and Rajadhyaksha, 2008). Indeed, calpain cleavage turns p25 into a more stable protein, which results in prolonged Cdk5 activity (Patrick et al., 1999). To examine whether mutant huntingtin altered the levels of p35 or its cleaved product p25, we performed immunoblot analysis using an antibody that recognizes either p35 or p25 forms (Fig. 5*A*). Our results showed a significant decrease in p35 levels in mutant STHdh^{Q111} cells compared with those observed in wild-type STHdh^{Q7} cells (~2-fold; $p \leq 0.001$). In contrast, the levels of p25, which were almost undetectable in wild-type STHdh^{Q7} striatal cells, were significantly higher in mutant STHdh^{Q111} cells (~2.5-fold; $p \leq 0.001$). Because p25 results from calpain activity, using Western blot we next measured the breakdown products of spectrin (SBDP), a well known calpain substrate that yields specific products at 150/160 kDa after calpain cleavage. Consistent with higher p25 accumulation, mutant STHdh^{Q111} cells exhibited increased levels of SBDP at 150/160 kDa compared with wild-type cells (~2-fold; $p \leq 0.05$) (Fig. 5*B*). Given that calpain activity is calcium dependent, and because of the fact that mutant STHdh^{Q111} cells exhibit at basal levels enhanced NMDAR activation (Gines et al., 2003; Seong et al., 2005), we next evaluated whether p25 accumulation might be a consequence of increased NMDAR-mediated calcium influx. To test this hypothesis, mutant huntingtin cells were treated with MK-801, a specific NMDAR antagonist that blocks calcium influx associated to NMDAR activation or with the calcium chelator EGTA. Immunoblot analysis revealed that p25 levels in mutant cells treated with MK-801 or EGTA were lower than those observed in untreated mutant cells (~1.2-fold decrease; $p \leq 0.01$), although still significantly higher compared with wild-type cells (~2.4-fold increase; $p \leq 0.001$) (Fig. 5*C*). Importantly, this reduction in p25 levels parallels the increase of p35 levels (~1.1-fold increase; $p \leq 0.01$) (Fig. 5*C*). These data suggest that endogenous activation of NMDAR in mutant striatal cells is not the major contributor to p25 accumulation.

We next evaluated whether either costimulation of NMDAR and D_1R or single activation induced higher accumulation of p25. Surprisingly, compared with untreated cells, all treatments failed to increase the accumulation of p25 any further in both wild-type and mutant striatal cells (Fig. 5*D–F*). These findings suggest that mutant huntingtin expression is sufficient to induce the conversion of p35 into p25 and support the idea that accumulation of p25 in parallel with higher Cdk5 activity may contribute to the increased vulnerability of mutant STHdh^{Q111} striatal cells to NMDA and D_1R activation.

Increased Cdk5 activity and tau phosphorylation in STHdh^{Q111} mutant cells

Our previous results have demonstrated higher phosphorylation of Cdk5 induced by D_1R activation alone or combined by preexposure to NMDA in mutant compared with wild-type striatal cells. To determine whether increased Cdk5 phosphorylation and accumulation of p25 was associated to higher Cdk5 activation, kinase activity was determined *in vitro* by using Cdk5 immunoprecipitated from untreated or treated (SKF38393 alone or combined with NMDA) wild-type STHdh^{Q7} and mutant STHdh^{Q111} striatal cells. Our results showed that at basal conditions mutant striatal cells exhibited a significant increase in Cdk5 activity compared with wild-type striatal cells (~2.5-fold; $p \leq 0.01$) (Fig. 6*A*). Interestingly, whereas NMDA exposure before SKF38393 treatment did not further increase Cdk5 activity in wild-type striatal

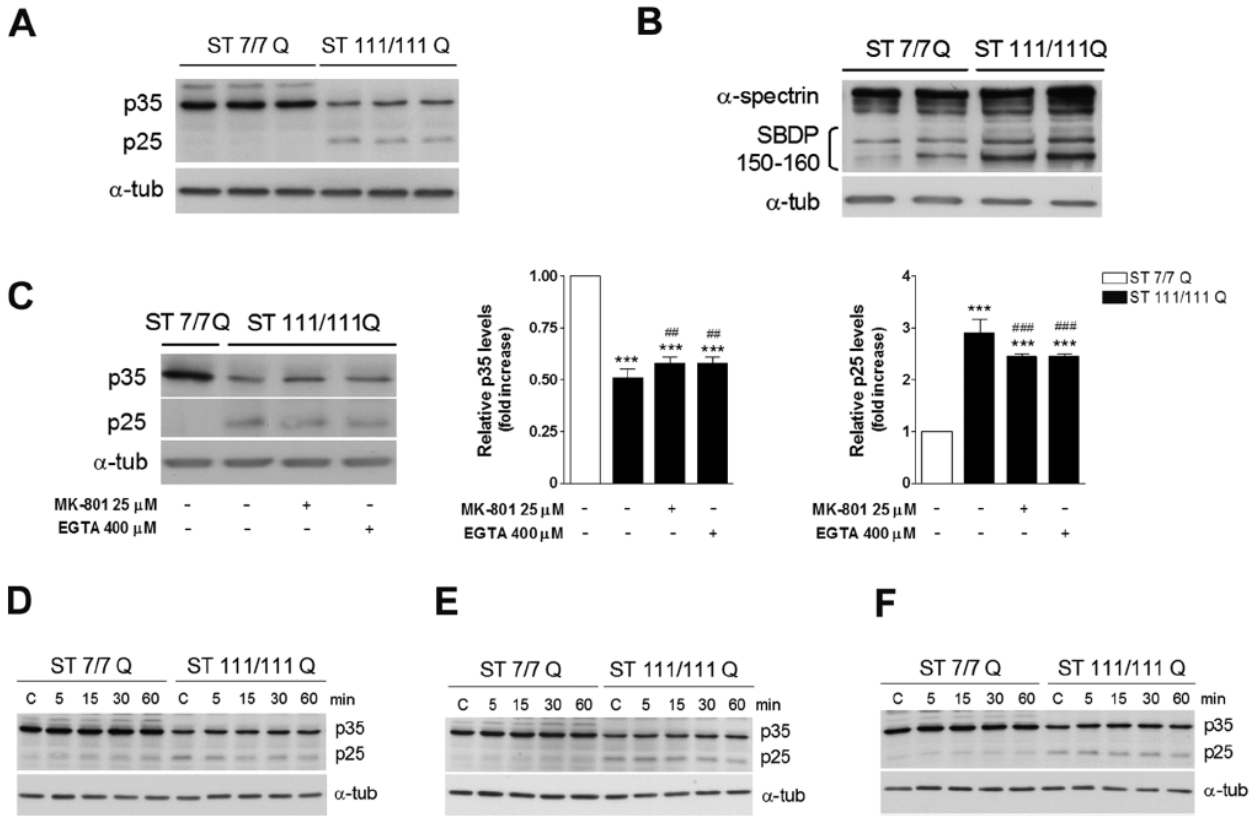

Figure 5. Increased p25/p35 levels in mutant STHdh^{Q111} striatal cells. ***A***, Representative Western blot showing levels of p35, p25, and α-tubulin as a loading control from wild-type (ST7/7Q) and mutant (ST111/111Q) striatal cells. ***B***, Representative Western blot showing α-spectrin and SDBP (150–160 kDa) and α-tubulin as a loading control from wild-type (ST7/7Q) and mutant (ST111/111Q) striatal cells. ***C***, Representative Western blot showing levels of p35, p25, and α-tubulin as a loading control from wild-type and mutant striatal cells treated with MK-801 25 μM or EGTA 400 μM for 6 h. The histograms represent the relative p35 and p25 levels expressed as fold increase versus wild-type cells. Values are given as mean ± SD of three independent experiments. ***$p <$ 0.001 mutant cells versus wild-type cells; $^{\#\#}p < 0.01$, $^{\#\#\#}p < 0.001$ treated versus vehicle-treated mutant cells as determined by one-way ANOVA followed by Bonferroni's multiple comparison test. ***D–F***, Representative Western blot showing p35 and p25 levels and α-tubulin as a loading control from wild-type and mutant striatal cells treated with NMDA 500 μM alone (***D***), SKF38393 100 μM alone (***E***), or pretreated with NMDA before SKF38393 exposure (***F***). Total extracts were obtained at different time periods (5, 15, 30, and 60 min) after treatment. ($n = 3$ independent experiments).

cells compared with SKF38393 alone (~1.2-fold and ~1.3-fold, respectively; $p = 0.53$), in mutant striatal cells NMDA significantly potentiates D_1R-induced Cdk5 activity (~1.9-fold, $p \leq 0.001$ and ~2.8-fold, $p \leq 0.001$, respectively) (Fig. 6*A*). In support of enhanced Cdk5 activity in mutant striatal cells, Western blot analysis using antibodies specific for phosphorylated tau (PHF-1, Ser^{396} and Ser^{404}) showed increased tau phosphorylation in basal mutant striatal cells compared with wild-type cells without changes on total tau levels (~1.5-fold increase; $p \leq 0.05$). Consistent with our results on Cdk5 activity, the levels of tau phosphorylation in wild-type cells pretreated with NMDA were similar than those detected in wild-type cells treated with SKF38393 alone (~1.2-fold increase and ~1.3-fold increase, respectively; $p = 0.97$) (Fig. 6*B*). In contrast, in mutant cells, higher levels of tau phosphorylation were detected when cells were pre-exposed to NMDA (~2.6-fold and ~2.1-fold, respectively; $p \leq 0.05$) (Fig. 6*B*). These data suggest that mutant huntingtin induces enhanced Cdk5 activity that results in increased phosphorylation of tau, an effect that is exacerbated by activation of D_1R alone or in combination with NMDAR.

Roscovitine ameliorates cell death evoked by SKF38393 and NMDA treatment in STHdh^{Q111} cells

The previous data suggest that Cdk5 may act as a down-stream mediator of NMDA and SKF38393 neurotoxicity in striatal cells. To test this hypothesis, we next evaluated the effect of roscovitine, a Cdk5 inhibitor, on NMDA and SKF38393-induced cell death. We found that roscovitine was able to significantly reverse the cell death induced by NMDA, SKF38393, or both in either wild-type and mutant huntingtin cells (Fig. 7). These findings demonstrate that a blockade of Cdk5 by roscovitine correlates with a reduction of cell death induced by NMDAR and D_1R activation in striatal cells and supports the involvement of aberrant Cdk5 activation in the increased vulnerability of mutant STHdh^{Q111} striatal cells to NMDA and SKF38393 treatment.

Cdk5 pathway is deregulated in *Hdh*^{Q111} knock-in mice and in HD human brain

To determine the relevance of deregulation of Cdk5 pathway in an *in vivo* HD model, we next analyzed whether Cdk5 alteration was also detected in the striatum of mutant *Hdh*^{Q111} mice. We first analyzed the levels of Cdk5 in striatal brain extracts obtained from mutant *Hdh*^{Q111} mice and wild-type *Hdh*^{Q7} littermate mice at 9 months of age. In agreement with our results on mutant striatal cells, immunoblot analysis revealed a significant increase in the ratio p-Tyr^{15} Cdk5/Cdk5 in the striatum of mutant *Hdh*^{Q111} mice compared with wild-type *Hdh*^{Q7} mice (~2-fold; $p \leq 0.05$) (Fig. 8*A*). Moreover, decreased p35 expression (~2-fold; $p \leq 0.01$) and higher accumulation of p25 forms (~2-fold; $p \leq 0.01$) were detected in

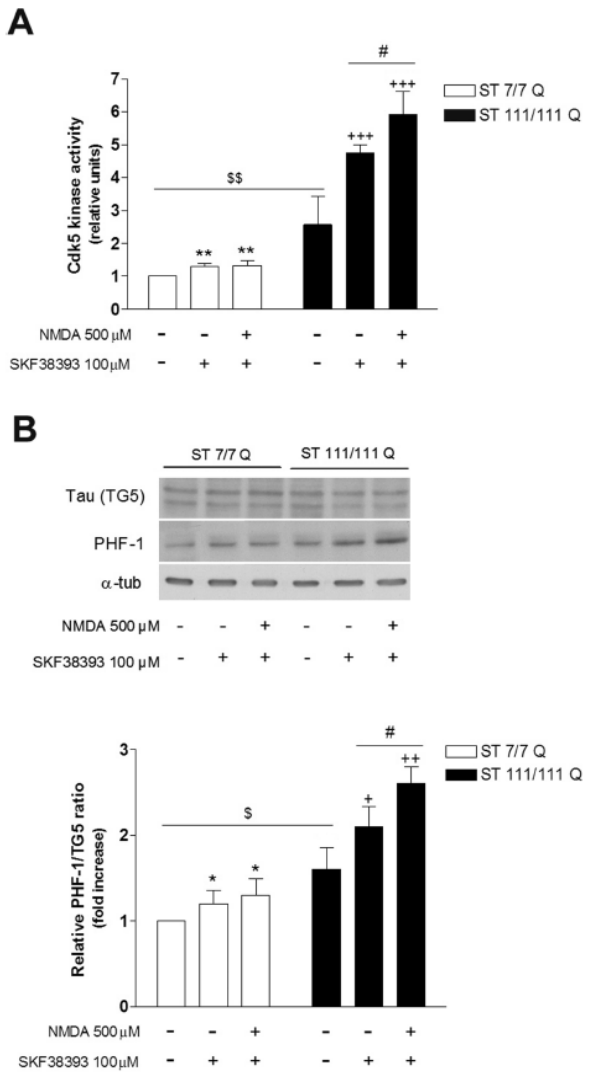

Figure 6. Mutant STHdh^{Q111} striatal cells exhibit increased Cdk5 activity associated with higher tau phosphorylation. Wild-type (ST7/7Q) and mutant (ST111/111Q) striatal cells were treated with SKF38393 (100 μM) or pretreated with NMDA (500 μM) before SKF38393 exposure, and total cell extracts were obtained 30 min after treatment. ***A***, *In vitro* kinase assay of immunoprecipitated Cdk5 from 500 μg of whole-cell lysates was performed using H1 peptide as substrate. The histogram represents the Cdk5 kinase activity in relative units corrected for the protein levels of Cdk5 for each sample and refereed to control (vehicle-treated) wild-type cells. Values are given as mean ± SD of three independent experiments. $^{**}p < 0.01$ treated versus vehicle-treated wild-type cells; $^{+++}p < 0.001$ treated versus vehicle-treated mutant cells; $^{\$\$}p < 0.01$ vehicle-treated mutant cells versus vehicle-treated wild-type cells; $^{\#}p < 0.05$ NMDA plus SKF38393-treated mutant cells versus SKF38393-treated mutant cells as determined by one-way ANOVA followed by Bonferroni's multiple comparison test. ***B***, Representative Western blot showing total Tau (TG5) levels, phosphorylated Tau (PHF-1) levels, and α-tubulin as a loading control from wild-type and mutant striatal cells. The histogram represents the relative PHF-1/TG5 ratio expressed as fold increase versus wild-type cells. Values are given as mean ± SD of three independent experiments. $^{*}p < 0.05$ treated versus vehicle-treated wild-type cells; $^{+}p < 0.05$, $^{++}p < 0.01$ treated versus vehicle-treated mutant cells; $^{\$}p < 0.05$ vehicle-treated mutant cells versus vehicle-treated wild-type cells; $^{\#}p < 0.05$ NMDA plus SKF38393-treated mutant cells versus SKF38393-treated mutant cells as determined by one-way ANOVA followed by Bonferroni's multiple comparison test.

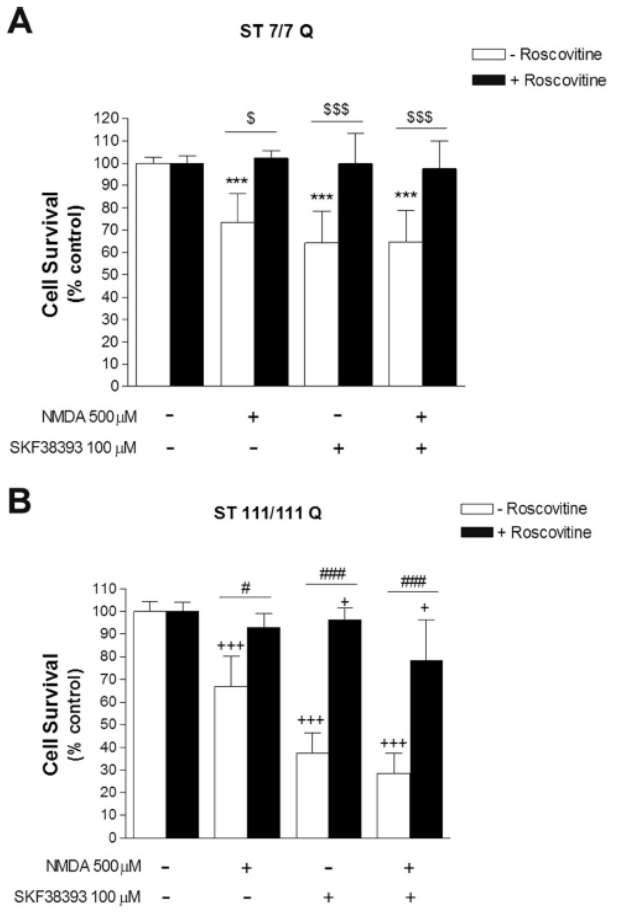

Figure 7. Inhibition of Cdk5 kinase activity by roscovitine ameliorates STHdh^{Q111} cells from cell death induced by SKF38393 and NMDA treatment. ***A***, ***B***, Wild-type (ST7/7Q; ***A***) and mutant (ST111/111Q; ***B***) striatal cells pretreated (1 h) with the Cdk5 inhibitor roscovitine (20 μM) were exposed to NMDA (500 μM) or SKF38393 (100 μM) alone, or preincubated with NMDA before SKF38393 exposure. Cell survival was evaluated 24 h later by scoring the percentage of Hoechst-stained nuclei. Forty fields were counted per condition per experiment, comprising at least 30–40 cells. Results are expressed as percentage of control (vehicle-treated) cells, and data are the mean ± SD of three independent experiments performed in triplicate. $^{***}p < 0.001$ treated versus vehicle-treated wild-type cells; $^{\$}p < 0.05$, $^{\$\$\$}p < 0.001$ roscovitine-treated versus roscovitine-untreated wild-type cells; $^{+}p < 0.05$, $^{+++}p < 0.001$ treated versus vehicle-treated mutant cells; $^{\#}p < 0.05$, $^{\#\#\#}p < 0.001$ roscovitine-treated versus roscovitine-untreated mutant cells as determined by one-way ANOVA followed by Bonferroni's multiple comparison test.

mutant *Hdh*^{Q111} striatal extracts compared with wild-type *Hdh*^{Q7} striatal extracts (Fig. 8*A*). Finally, to determine whether increased Cdk5 phosphorylation and p25 expression involved higher Cdk5 activity, we next examined the levels of tau phosphorylation. Western blot analysis revealed a significant increase of tau phosphorylation (PHF-1) in mutant *Hdh*^{Q111} striatal brain compared with wild-type *Hdh*^{Q7} striatal brain (~2-fold; $p \leq 0.01$) (Fig. 8*B*). These results suggest that mutant huntingtin expression enhances Cdk5 activity *in vivo* by increasing Cdk5 phosphorylation and the conversion of p35 to p25, which results in aberrant phosphorylation of tau protein. Finally, we also investigated whether aberrant Cdk5 pathway was manifested in HD human brain. Western blot analysis confirmed a decrease of Cdk5 in human striatal brain samples from HD patients compared with control brains (Fig. 8*C*). Unfortunately, we failed to detect Cdk5 phosphorylation (Tyr15) in human brain extracts probably because of the sensitivity of this phosphorylation site to postmortem intervals (range from 4 to 15 h for HD samples and from 4 to 23 h for control samples). Importantly, an increase of p25/p35 levels

were also detected in HD human striatal brains compared with control striatal brains. Thus, HD striatal brains exhibited a significant decrease in p35 expression (~3-fold; $p \leq 0.05$) and increased p25 levels (~4-fold; $p \leq 0.001$) (Fig. 8*C*) compared with control striatal brains. These data support the view that aberrant Cdk5 pathway is also manifested in HD patients and suggest a role of p25/Cdk5 in HD pathology.

Discussion

Degeneration of medium spiny neurons in the striatum is the main hallmark of HD neuropathology. However, the molecular mechanism by which mutant huntingtin toxicity causes such specific cell death remains unknown. Our present work demonstrates that full-length mutant huntingtin enhances the sensitivity of striatal cells to dopamine leading to increased neuronal death. This effect on neurotoxicity is mediated by D_1 but not D_2 receptors as demonstrated by using specific dopamine-receptor agonists. Thus, the direct activation of D_1R by SKF38393 revealed a higher dose–response reduction in cell survival in mutant STHdh^{Q111} than in wild-type STHdh^{Q7} cells, an effect that was mostly reverted by the selective D_1 antagonist SCH23390. The lack of cell death in the presence of the D_2 agonist quinpirole indicates that the neurotoxic effect of dopamine in knock-in mutant striatal cells is mainly associated with D_1R activation. These results agree with previous reports indicating the role of D_1R in striatal neuronal loss. It has been proposed that dopamine, by acting through activation of D_1R and auto-oxidation, causes striatal neurotoxicity by inducing the neuronal expression and activity of inducible nitric oxide synthase (Wersinger et al., 2004). Moreover, dopamine through D_1R potentiates glutamate-induced toxicity in cultured striatal cells from *YAC128* HD mice (Tang et al., 2007). However, the involvement of D_2R in HD pathology cannot be completely ruled out because dopamine via D_2 receptors enhances mutant huntingtin aggregation and mitochondrial dysfunction in exon-1 HD mouse models (Charvin et al., 2005; Benchoua et al., 2008). Therefore, it is possible that at early disease stages that is in the absence of mutant huntingtin cleavage and aggregate formation, dopamine toxicity acts primarily via D_1R whereas later in the disease progress altered D_1 and D_2 receptor signaling contribute to HD pathology.

It is well known that glutamate and dopamine receptors regulate striatal neuronal function by interacting and modulating each other. Specifically, an association between NMDAR and D_1R has been reported, although the nature of this interaction remains unclear (Scott et al., 2002; Salter, 2003; Cepeda and Levine, 2006; Missale et al., 2006). Here, we have demonstrated that NMDA potentiates D_1R-induced cell death in mutant STHdh^{Q111} cells but not in wild-type STHdh^{Q7} cells. We have tested toxic NMDA concentrations, which induce similar cell death in wild-type and mutant cells and low NMDA concentrations,

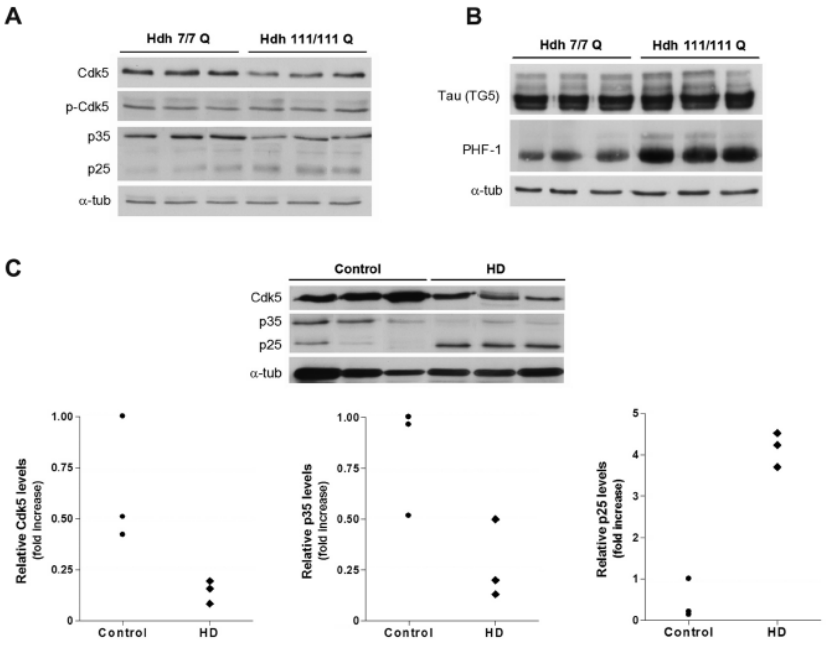

Figure 8. Cdk5 pathway is altered in HD knock-in mice and HD human brain. ***A***, Representative Western blot showing levels of p-Cdk5, Cdk5, p35, p25, and α-tubulin as a loading control from striatal extracts of wild-type *Hdh*^{Q7} and mutant *Hdh*^{Q111} mice at 9 months of age. ***B***, Representative Western blot showing levels of total Tau (TG5), phosphorylated Tau (PHF-1), and α-tubulin as a loading control from striatal extracts of wild-type *Hdh*^{Q7} and mutant *Hdh*^{Q111} mice at 9 months of age. Values are given as mean ± SD of three independent samples. $^{**}p < 0.01$ as determined by Student's *t* test. ***C***, Representative Western blot showing levels of total Cdk5, p35, p25, and α-tubulin as a loading control from human brain striatal samples of control ($n = 3$) and HD patients ($n = 3$). Scatter plots represent the relative levels of Cdk5, p35, and p25. The higher value obtained in control brain extracts was set as 1.

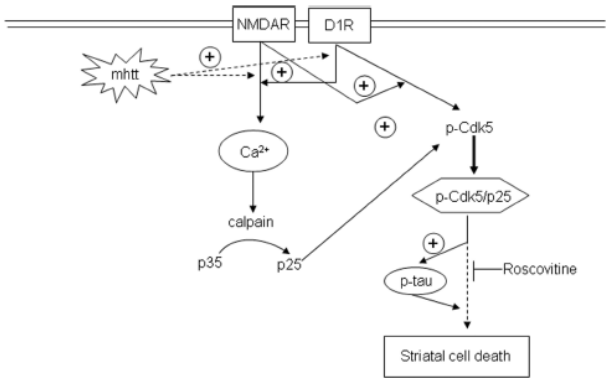

Figure 9. Increased sensitivity of mutant huntingtin striatal cells to glutamate and dopamine receptor activation involves enhanced Cdk5 activity. Hypothetical model to depict the link between neurotoxicity induced by dopamine and glutamate receptor activation and the Cdk5 pathway in HD. Enhanced activation of NMDAR and D_1R induced by mutant huntingtin leads to deregulation of calcium homeostasis (Cepeda et al., 2001; Seong et al., 2005; Starling et al., 2005; Tang et al., 2007). Increased intracellular calcium in turn leads to higher calpain activity that results in enhanced cleavage of p35 into p25 (Lee et al., 2000). In addition, as our data demonstrate, activation of NMDAR may potentiate D_1R-mediated phosphorylation of Cdk5 at Tyr^{15}, which has been shown to regulate Cdk5-induced neurotoxicity (Lin et al., 2007). The generation of p-Cdk5/p25 complexes implies Cdk5 hyperactivation that is responsible for the phosphorylation of new substrates such as tau protein. Now, hyperphosphorylation of tau in concert with unknown yet down-stream p25/Cdk5 effectors might contribute to striatal cell death and dysfunction and therefore to HD neuropathology. The model is supported by the capacity of roscovitine, a Cdk5 inhibitor, to prevent cellular death induced by NMDAR and D_1R activation.

which, per se, are not toxic (Xifró et al., 2008). Notably, either toxic or subtoxic NMDA concentrations enhanced the effect in cell death mediated by SKF38393 only in mutant STHdh^{Q111} cells. These results agree with previous studies showing that glutamate and dopamine act synergistically to induce degeneration of striatal cells in *YAC128* HD mouse models (Tang et al., 2007). Altogether, our data suggest that mutant huntingtin alters the dopaminergic and glutamatergic signaling not only by affecting NMDAR and D_1R but also by altering the cross-talk between both pathways. Consequently, to gain a better understanding of how mutant huntingtin increases the vulnerability of striatal cells to neurotoxicity, we focused on defining the molecular mechanisms that underlie the toxic effect of NMDAR and D_1R activation on striatal cell survival.

Recent studies have identified Cdk5 as mediator of dopaminergic neuronal loss in mouse models of Parkinson's disease because inhibition of Cdk5 reduces neurodegeneration and behavior disturbances in these mouse models (Smith et al., 2003, 2006; Przedborski, 2007). Moreover, it has been demonstrated that Cdk5 can regulate NMDAR signaling by direct phosphorylation of NR2A and NR2B subunits or indirectly via phosphorylation of postsynaptic density-95 (Morabito et al., 2004; Zhang et al., 2008). Therefore, it is reasonable to hypothesize a role for Cdk5 in the increased vulnerability of mutant huntingtin striatal cells to NMDAR and D_1R activation.

We have examined two important features of Cdk5 activation related to its pro-apoptotic function: the levels of Tyr^{15} phosphorylation (Lin et al., 2007) and the accumulation of p25 as a result of calpain-mediated p35 cleavage (Kusakawa et al., 2000; Lee et al., 2000). Our results in knock-in striatal cells define a new role of mutant huntingtin as modulator of the Cdk5 pathway by (1) decreasing Cdk5 expression and increasing the levels of phosphorylated Tyr^{15}-Cdk5 and (2) by increasing the conversion of p35 into p25, which in turn results in enhanced Cdk5 activity. Moreover, we have demonstrated a polyQ-dependent reduction of Cdk5 expression together with an increase in Tyr^{15}-Cdk5 phosphorylation in striatal cells. These data support the idea of a direct role of mutant huntingtin in Cdk5 changes rather than a secondary consequence of mutant huntingtin toxicity. Consistent with the results obtained in the knock-in striatal cell line, we also found deregulation of Cdk5 in *Hdh*^{Q111} knock-in mice and HD human brain. Our studies demonstrate an increased of p-Tyr^{15}-Cdk5/Cdk5 ratio and a significant accumulation of p25 together with reduced p35 expression in the striatum of *Hdh*^{Q111} mutant mice and HD human brain. In agreement with these results, Anne et al. (2007) have reported reduced levels of Cdk5 and p35 in HD human brain, although no data on p25 accumulation was reported. These data are relevant because it has been demonstrated a protective role of p35/Cdk5 complexes in HD. Phosphorylation of mutant huntingtin by p35/Cdk5 complexes reduces huntingtin cleavage by caspases resulting in attenuated aggregate formation and toxicity (Luo et al., 2005). Moreover, phosphorylation of wild-type huntingtin by Cdk5 protects striatal cells against DNA damage (Anne et al., 2007). Both reports speculate that loss of p35/Cdk5 function may have detrimental consequences for HD pathology. Therefore, our novel results demonstrating an accumulation of p25 in HD mouse brain and striatal cell models and in HD human brain might be relevant to explain the apparent dual role of Cdk5 in HD pathology. Indeed, it is well established the role of p25 as a cell death inductor (Cruz and Tsai, 2004; Dhariwala and Rajadhyaksha, 2008). Thus, neurotoxicity induced by β-amyloid, ischemia, or MPTP causes aberrant Cdk5 activity through the generation and accumulation of p25 (Cruz and Tsai, 2004; Dhariwala and Rajadhyaksha, 2008). Furthermore, this truncated p25 form relocalizes Cdk5 activity with the consequent alteration of Cdk5 substrate specificity (Patrick et al., 1999; Ko et al., 2001; Bian et al., 2002). Actually, elevated Cdk5 activity accumulation of p25 and hyperphosphorylated tau have been described in brain of AD patients (Cruz and Tsai, 2004; Dhariwala and Rajadhyaksha, 2008). Notably, our studies have identified tau as a downstream target of aberrant Cdk5 activity in HD mouse and striatal cell models. The specific role of tau in HD pathology remains to be elucidated. However, given evidence of impaired axonal trafficking in HD (Truant et al., 2006), it seems reasonable to speculate that altered tau may be involved in the vesicular trafficking deficiencies associated to HD pathology.

Collectively, our results clearly demonstrate that mutant huntingtin deregulates Cdk5 pathway. However, one important question is to determine whether aberrant Cdk5 activity plays a role in the increased sensitivity of mutant huntingtin cells to NMDAR and D_1R activation. Indeed, our data indicate that deregulated Cdk5 pathway might be instrumental in the HD neurodegenerative process by increasing the vulnerability of striatal cells to dopamine and glutamate inputs. This conclusion is supported by the following observations: first, SKF38393 induced higher Cdk5 phosphorylation and activity in mutant cells than in wild-type cells. Second, exposure of mutant cells to NMDA before SKF38393 induced higher levels of Cdk5 phosphorylation and activity than in wild-type cells or mutant cells treated with SKF38393 alone. Third, compared with wild-type cells, increased levels of phosphorylated tau were detected in mutant striatal cells treated with SKF38393 alone or pre-exposed to NMDA. Therefore, these data demonstrate that mutant huntingtin increases the sensitivity of striatal cells to dopamine and glutamate inputs by altering a common NMDAR and D_1R downstream pathway such is Cdk5. Supporting this conclusion are the findings that the inhibition of Cdk5 activity by roscovitine mainly prevented striatal cell death induced by NMDA, SKF38393, or both. However, because neuronal loss induced by NMDA and SKF38393 cotreatment was not fully prevented by roscovitine in mutant cells, we can speculate that additional mechanism independent of Cdk5 might be involved in the toxicity associated to NMDAR and D_1R activation.

Based on these findings, an attractive model of striatal cell death is one in which aberrant Cdk5 activity (Fig. 6) as a result of enhanced Cdk5 phosphorylation at Tyr^{15} (Fig. 4) and p25 accumulation (Fig. 5) might sensitize mutant huntingtin striatal cells to NMDAR and D_1R activation. Therefore, once NMDAR and D_1R were activated, both receptors might act coordinately to promote calcium homeostasis deregulation (Cepeda et al., 2001; Starling et al., 2005; Tang et al., 2007) with the consequent mitochondrial depolarization and caspase activation (Zeron et al., 2002, 2004). In addition, as our data demonstrate, the activation of NMDAR may further potentiate D_1R-mediated phosphorylation of Cdk5, leading to the generation of p-Cdk5/p25 complexes and enhanced Cdk5 activity. Sustained Cdk5 activity may now target for phosphorylation different substrates such as tau or additional recognized Cdk5 effectors (Gong et al., 2003; Lee et al., 2007) and contribute to striatal cell death in HD.

In conclusion, our results provide evidence that aberrant Cdk5 activity is involved in the increased sensitivity of mutant

huntingtin striatal cells to dopamine and glutamate inputs and reveal p25/Cdk5 complexes as potential candidates for future pharmacological intervention in HD (Fig. 9).

References

Akashiba H, Ikegaya Y, Nishiyama N, Matsuki N (2008) Differential involvement of cell cycle reactivation between striatal and cortical neurons in cell death induced by 3-nitropropionic acid. J Biol Chem 283:6594–6606.

Anne SL, Saudou F, Humbert S (2007) Phosphorylation of huntingtin by cyclin-dependent kinase 5 is induced by DNA damage and regulates wild-type and mutant huntingtin toxicity in neurons. J Neurosci 27:7318–7328.

Beal MF, Brouillet E, Jenkins BG, Ferrante RJ, Kowall NW, Miller JM, Storey E, Srivastava R, Rosen BR, Hyman BT (1993) Neurochemical and histologic characterization of striatal excitotoxic lesions produced by the mitochondrial toxin 3-nitropropionic acid. J Neurosci 13:4181–4192.

Benchoua A, Trioulier Y, Diguet E, Malgorn C, Gaillard MC, Dufour N, Elalouf JM, Krajewski S, Hantraye P, Déglon N, Brouillet E (2008) Dopamine determines the vulnerability of striatal neurons to the N-terminal fragment of mutant huntingtin through the regulation of mitochondrial complex II. Hum Mol Genet 17:1446–1456.

Bian F, Nath R, Sobocinski G, Booher RN, Lipinski WJ, Callahan MJ, Pack A, Wang KK, Walker LC (2002) Axonopathy, tau abnormalities and dyskinesia, but no neurofibrillary tangles in p25-transgenic mice. J Comp Neurol 446:257–266.

Brecht S, Kirchhof R, Chromik A, Willesen M, Nicolaus T, Raivich G, Wessig J, Waetzig V, Goetz M, Claussen M, Pearse D, Kuan CY, Vaudano E, Behrens A, Wagner E, Flavell RA, Davis RJ, Herdegen T (2005) Specific pathophysiological functions of JNK isoforms in the brain. Eur J Neurosci 21:363–377.

Centeno C, Repici M, Chatton JY, Riederer BM, Bonny C, Nicod P, Price M, Clarke PG, Papa S, Franzoso G, Borsello T (2007) Role of the JNK pathway in NMDA-mediated excitotoxicity of cortical neurons. Cell Death Differ 14:240–253.

Cepeda C, Levine MS (2006) Where do you think you are going? The NMDA-D_1 receptor trap. Sci STKE: 333:pe20.

Cepeda C, Ariano MA, Calvert CR, Flores-Hernández J, Chandler SH, Leavitt BR, Hayden MR, Levine MS (2001) NMDA receptor function in mouse models of Huntington disease. J Neurosci Res 66:525–539.

Charvin D, Vanhoutte P, Pagès C, Borrelli E, Borelli E, Caboche J (2005) Unraveling a role for dopamine in Huntington's disease: the dual role of reactive oxygen species and D_2 receptor stimulation. Proc Natl Acad Sci U S A 102:12218–12223.

Crespo-Biel N, Camins A, Pelegrí C, Vilaplana J, Pallàs M, Canudas AM (2007) 3-Nitropropionic acid activates calpain/cdk5 pathway in rat striatum. Neurosci Lett 421:77–81.

Cruz JC, Tsai LH (2004) A Jekyll and Hyde kinase: roles for Cdk5 in brain development and disease. Curr Opin Neurobiol 14:390–394.

Cyr M, Sotnikova TD, Gainetdinov RR, Caron MG (2006) Dopamine enhances motor and neuropathological consequences of polyglutamine expanded huntingtin. FASEB J 20:2541–2543.

de la Monte SM, Vonsattel JP, Richardson EP Jr (1988) Morphometric demonstration of atrophic changes in the cerebral cortex, white matter, and neostriatum in Huntington's disease. J Neuropathol Exp Neurol 47:516–525.

Dhariwala FA, Rajadhyaksha MS (2008) An unusual member of the cdk family: cdk5. Cell Mol Neurobiol 28:351–369.

Fan MM, Raymond LA (2007) N-methyl-D-aspartate (NMDA) receptor function and excitotoxicity in Huntington's disease. Prog Neurobiol 81:272–293.

Gines S, Ivanova E, Seong IS, Saura CA, MacDonald ME (2003) Enhanced Akt signaling is an early pro-survival response that reflects N-methyl-D-aspartate receptor activation in Huntington's disease knock-in striatal cells. J Biol Chem 278:50514–50522.

Gong X, Tang X, Wiedmann M, Wang X, Peng J, Zheng D, Blair LA, Marshall J, Mao Z (2003) Cdk5-mediated inhibition of the protective effects of transcription factor MEF2 in neurotoxicity-induced apoptosis. Neuron 38:33–46.

Jakel RJ, Maragos WF (2000) Neuronal cell death in Huntington's disease: a potential role for dopamine. Trends Neurosci 23:239–245.

Kazantsev A, Preisinger E, Dranovsky A, Goldgaber D, Housman D (1999) Insoluble detergent-resistant aggregates form between pathological and nonpathological lengths of polyglutamine in mammalian cells. Proc Natl Acad Sci U S A 96:11404–11409.

Ko J, Humbert S, Bronson RT, Takahashi S, Kulkarni AB, Li E, Tsai LH (2001) p35 and p39 are essential for cyclin-dependent kinase 5 function during neurodevelopment. J Neurosci 21:6758–6771.

Kusakawa G, Saito T, Onuki R, Ishiguro K, Kishimoto T, Hisanaga S (2000) Calpain-dependent proteolitic cleavage of the p35 cyclin-dependent kinase 5 activator to p25. J Biol Chem 275:17166–17172.

Lee JH, Kim HS, Lee SJ, Kim KT (2007) Stabilization and activation of p53 induced by Cdk5 contributes to neuronal cell death. J Cell Sci 120:2259–2271.

Lee MS, Kwon YT, Li M, Peng J, Friedlander RM, Tsai LH (2000) Neurotoxicity induces cleavage of p35 to p25 by calpain. Nature 405:360–364.

Lin H, Lin TY, Juang JL (2007) Abl deregulates Cdk5 kinase activity and subcellular localization in *Drosophila* neurodegeneration. Cell Death Differ 14:607–615.

Luo S, Vacher C, Davies JE, Rubinsztein DC (2005) Cdk5 phosphorylation of huntingtin reduces its cleavage by caspases: implications for mutant huntingtin toxicity. J Cell Biol 169:647–656.

MacDonald ME, Gines S, Gusella JF, Wheeler VC (2003) Huntington's disease. Neuromolecular Med 4:7–20.

Martin JB, Gusella JF (1986) Huntington's disease. Pathogenesis and management. N Engl J Med 315:1267–1276.

Missale C, Fiorentini C, Busi C, Collo G, Spano PF (2006) The NMDA/D_1 receptor complex as a new target in drug development. Curr Top Med Chem 6:801–808.

Morabito MA, Sheng M, Tsai LH (2004) Cyclin-dependent kinase 5 phosphorylates the N-terminal domain of the postsynaptic density protein PSD-95 in neurons. J Neurosci 24:865–876.

Patrick GN, Zukerberg L, Nikolic M, de la Monte S, Dikkes P, Tsai LH (1999) Conversion of p35 to p25 deregulates Cdk5 activity and promotes neurodegeneration. Nature 402:615–622.

Pérez-Navarro E, Canals JM, Ginés S, Alberch J (2006) Cellular and molecular mechanisms involved in the selective vulnerability of striatal projection neurons in Huntington's disease. Histol Histopathol 21:1217–1232.

Przedborski S (2007) Peroxiredoxin-2 links Cdk5 to neurodegeneration. Nat Med 13:907–909.

Salter MW (2003) D_1 and NMDA receptor hook up: expanding on an emerging theme. Trends Neurosci 26:235–237.

Scott L, Kruse MS, Forssberg H, Brismar H, Greengard P, Aperia A (2002) Selective up-regulation of dopamine D_1 receptors in dendritic spines by NMDA receptor activation. Proc Natl Acad Sci U S A 99:1661–1664.

Seong IS, Ivanova E, Lee JM, Choo YS, Fossale E, Anderson M, Gusella JF, Laramie JM, Myers RH, Lesort M, MacDonald ME (2005) HD CAG repeat implicates a dominant property of huntingtin in mitochondrial energy metabolism. Hum Mol Genet 14:2871–2880.

Smith PD, Crocker SJ, Jackson-Lewis V, Jordan-Sciutto KL, Hayley S, Mount MP, O'Hare MJ, Callaghan S, Slack RS, Przedborski S, Anisman H, Park DS (2003) Cyclin-dependent kinase 5 is a mediator of dopaminergic neuron loss in a mouse model of Parkinson's disease. Proc Natl Acad Sci U S A 100:13650–13655.

Smith PD, Mount MP, Shree R, Callaghan S, Slack RS, Anisman H, Vincent I, Wang X, Mao Z, Park DS (2006) Calpain-regulated p35/cdk5 plays a central role in dopaminergic neuron death through modulation of the transcription factor myocyte enhancer factor 2. J Neurosci 26:440–447.

Starling AJ, André VM, Cepeda C, de Lima M, Chandler SH, Levine MS (2005) Alterations in N-methyl-D-aspartate receptor sensitivity and magnesium blockade occur early in development in the R6/2 mouse model of Huntington's disease. J Neurosci Res 82:377–386.

Tang TS, Chen X, Liu J, Bezprozvanny I (2007) Dopaminergic signaling and striatal neurodegeneration in Huntington's disease. J Neurosci 27:7899–7910.

Trettel F, Rigamonti D, Hilditch-Maguire P, Wheeler VC, Sharp AH, Persichetti F, Cattaneo E, MacDonald ME (2000) Dominant phenotypes produced by the HD mutation in STHdh(Q111) striatal cells. Hum Mol Genet 9:2799–2809.

Truant R, Atwal R, Burtnik A (2006) Hypothesis: Huntingtin may function in membrane association and vesicular trafficking. Biochem Cell Biol 84:912–917.

Wersinger C, Chen J, Sidhu A (2004) Bimodal induction of dopamine-mediated striatal neurotoxicity is mediated through both activation of D_1 dopamine receptors and autoxidation. Mol Cell Neurosci 25:124–137.

Wheeler VC, Auerbach W, White JK, Srinidhi J, Auerbach A, Ryan A, Duyao MP, Vrbanac V, Weaver M, Gusella JF, Joyner AL, MacDonald ME (1999) Length-dependent gametic CAG repeat instability in the Huntington's disease knock-in mouse. Hum Mol Genet 8:115–122.

Xifró X, García-Martínez JM, Del Toro D, Alberch J, Pérez-Navarro E (2008) Calcineurin is involved in the early activation of NMDA-mediated cell death in mutant huntingtin knock-in striatal cells. J Neurochem 105:1596–1612.

Zeron MM, Hansson O, Chen N, Wellington CL, Leavitt BR, Brundin P, Hayden MR, Raymond LA (2002) Increased sensitivity to N-methyl-D-aspartate receptor-mediated excitotoxicity in a mouse model of Huntington's disease. Neuron 33:849–860.

Zeron MM, Fernandes HB, Krebs C, Shehadeh J, Wellington CL, Leavitt BR, Baimbridge KG, Hayden MR, Raymond LA (2004) Potentiation of NMDA receptor-mediated excitotoxicity linked with intrinsic apoptotic pathway in YAC transgenic mouse model of Huntington's disease. Mol Cell Neurosci 25:469–479.

Zhang S, Edelmann L, Liu J, Crandall JE, Morabito MA (2008) Cdk5 regulates the phosphorylation of tyrosine 1472 NR2B and the surface expression of NMDA receptors. J Neurosci 28:415–424.

SEGUNDO TRABAJO: “Impaired TrkB-mediated ERK1/2 activation in Huntington’s disease knock-in striatal cells involves reduced p52/p46 Shc expression”

Publicado en The Journal of Biological Chemistry 2010, May 4.

2.- Caracterización de las vías intracelulares activadas tras la estimulación del receptor TrkB con BDNF en modelos celulares *knock-in* de la enfermedad de Huntington.

2.1.- Estudiar si la alteración en los niveles del receptor TrkB asociada a la expresión de la htt mutada se traduce en una anómala señalización intracelular en respuesta a BDNF.

2.2.- Estudiar la implicación de una anómala señalización intracelular del receptor TrkB en la mayor susceptibilidad estriatal frente a estrés oxidativo en modelos celulares *knock-in* de la enfermedad de Huntington.

En este estudio se analizó si la alteración en los niveles del receptor TrkB asociada a la expresión de la htt mutada se traduce en una anómala señalización intracelular en respuesta a BDNF. El resultado más relevante ha sido constatar que en presencia de la htt mutada la vía de señalización de TrkB-ERK1/2 se encuentra alterada de manera específica, debido a una reducida expresión de las proteínas acopladoras p52/p46Shc. La menor activación de esta vía intracelular conlleva una mayor susceptibilidad de las células estriatales frente a un estímulo de estrés oxidativo inducido con H_2O_2.

JBC Papers in Press. Published on May 4, 2010 as Manuscript M109.084202
The latest version is at http://www.jbc.org/cgi/doi/10.1074/jbc.M109.084202

IMPAIRED TRKB-MEDIATED ERK1/2 ACTIVATION IN HUNTINGTON'S DISEASE KNOCK-IN STRIATAL CELLS INVOLVES REDUCED P52/P46 SHC EXPRESSION

Silvia Ginés[1,2], Paola Paoletti[1,2], Jordi Alberch[1,2]
From the [1] Departament de Biologia Cel.lular, Immunologia i Neurociències, Facultat de Medicina, Institut d´Investigacions Biomèdiques August Pi i Sunyer (IDIBAPS). Universitat de Barcelona, Casanova 143, E-08036 Barcelona, Spain and [2] Centro de Investigación Biomédica en Red sobre Enfermedades Neurodegenerativas (CIBERNED)

Running head. Disrupted BDNF-mediated ERK1/2 activation in HD.

Address correspondence: Silvia Ginés, Universitat de Barcelona, Casanova 143, E-08036 Barcelona, Spain. Phone: +34-93-4035284. Fax: +34-93-4021907. E-mail: silviagines@ub.edu

Altered neurotrophic support as a result of reduced BDNF expression and trafficking has been revealed as a key factor in Huntington's disease (HD) pathology. BDNF binds to and activates the tyrosine kinase receptor TrkB leading to activation of intracellular signaling pathways to promote differentiation and cell survival. In order to design new neuroprotective therapies based on BDNF delivery it is important to define whether BDNF-mediated TrkB signaling is affected in HD. Here, we demonstrate reduced TrkB-mediated Ras/MAPK/ERK1/2 signaling but unchanged PI3K/Akt and PLC-γ activation in knock-in HD striatal cells. Altered BDNF-mediated ERK1/2 activation in mutant huntingtin cells is associated with reduced expression of p52/p46 Shc docking proteins. Notably, reduced BDNF-induced ERK1/2 activation increases the sensitivity of mutant huntingtin striatal cells to oxidative damage. Accordingly, pharmacological activation of the MAPK pathway with PMA prevents cell death induced by oxidative stress. Taken together our results suggest that in addition to reduced BDNF, diminished Ras/MAPK/ERK1/2 activation is involved in neurotrophic deficits associated with HD pathology. Therefore pharmacological approaches aimed to directly modulate the MAPK/ERK1/2 pathway may represent a valuable therapeutic strategy in HD.

Trophic factors have been suggested as therapeutic candidates for the treatment of several neurodegenerative diseases given that they are essential contributors for maintenance of neuronal survival and differentiation. A number of studies have focused on the study of BDNF and its role in HD as striatal neurons, the most prominently neurons affected in HD, require BDNF for their normal function and survival (1-4). Thus, recent evidence demonstrate that wild-type huntingtin facilitates BDNF transcription whereas mutant huntingtin impairs it (5;6). Accordingly, BDNF mRNA expression and protein levels are reduced in cortex and striatum of HD patients and in mouse and cellular models of HD (7-10). In order to respond to BDNF, striatal neurons must exhibit an appropriate expression and function of its high affinity receptor TrkB. Notably, we have previously described a significant reduction of total TrkB receptors in several HD mouse models, HD knock-in cells as well as in HD human brain (11). Moreover, reduced TrkB mRNA levels were also found in caudate but not in the cortex of HD patients (10). These results suggest that altered neurotrophic support as a result of BDNF deficit may contribute to the selective degeneration of striatal neurons in HD. However, no study has been reported on the functional consequences of TrkB down-regulation in HD pathology. The neuroprotective action of BDNF through TrkB receptors is associated with activation of the mitogen-activated protein kinase (MAPKs), the phosphatidylinositol 3-kinase (PI3K)/Akt and the PLC-γ pathways (12-14). We therefore, examined in a genetically precise HD cell model: immortalized STHdh^{Q111} striatal neuronal cells derived from Hdh^{Q111} embryos (9;15) whether altered TrkB levels associated with mutant huntingtin expression involve altered BDNF signaling. We found in mutant huntingtin striatal cells a defective BDNF-mediated Ras-MAPK-ERK1/2 activation but unaffected BDNF-induced PI3K-Akt and PLC-γ signaling. We provide evidence that diminished levels of

p52/46 adapter proteins rather than decreased cell-surface TrkB receptor *per se* may account for the reduced BDNF-mediated ERK1/2 activation. Finally, the functional relevance of altered BDNF-induced ERK1/2 activation in mutant cells was demonstrated by analysis of cell death and dysfunction induced by oxidative stress. Based on these data, we propose that pharmacological modulation of ERK1/2 pathway may provide a new therapeutic target in HD.

Experimental Procedures

Chemicals and reagents- BDNF (Peprotech EC Ltd., London UK), EGF (R&D System, USA), Phorbol 12-myristate 13-acetate (PMA) were obtained from Sigma-Aldrich (St Louis, MO, USA), PD098059 was purchased from Calbiochem (San Diego, CA). Phospho p44/42 ERK1/2 (Thr202/Tyr204), Phospho-MEK1/2 (Ser217/221), Phospho-c-Raf (Ser338), Phospho-Akt (Ser473), Phospho-PLC-γ (Tyr783), total ERK1/2, total MEK1/2, total c-Raf, total Akt and total PLC-γ were obtained from Cell Signaling Technology (Beverly, MA). TrkB polyclonal antibody that only recognizes the full-length TrkB isoform (sc-7268; C-tal epitope) and phospho-Trk (detects Trk phosphorylated at Tyr 496/490) (sc-8058) were obtained from Santa Cruz Biotechnology (Santa Cruz, CA, USA). TrkB polyclonal antibody that recognizes the extracellular domain of TrkB, IRS-1 polyclonal antibody, p52/46Shc and p66Shc polyclonal antibodies were obtained from Millipore (Billerica, MA, USA). Ras monoclonal antibody was purchased from BD Bioscience (San Jose, CA USA). Anti-HA (Sigma-Aldrich), TRITC (tetramethylrhodamine isothiocyanate)-phalloidin and α-tubulin were purchased from Sigma-Aldrich (St. Louis, MO).

Cell cultures- Conditionally immortalized wild-type STHdh^{Q7} and mutant STHdh^{Q111} striatal neuronal progenitor cell lines expressing endogenous levels of normal and mutant full-length huntingtin with 7 and 111 glutamines, respectively, were generated from wild-type *Hdh*^{Q7} and homozygous *Hdh*^{Q111} littermate embryos (9;15). The knock-in striatal models represent faithfully the HD mutation carried by patients since elongated polyglutamine tracts are placed within the correct context of the murine *Hdh* gene. Thus, immortalized striatal cells accurately express normal and mutant huntingtin and do not exhibit amino terminal inclusions which allow us to study changes involved in early HD pathogenesis (15). Striatal cells were grown at 33ºC in Dulbecco's modified Eagle's medium (DMEM; Sigma-Aldrich) supplemented with 10 % fetal bovine serum (FBS), 1 % streptomycin-penicillin, 2 mM L-glutamine, 1 mM sodium pyruvate and 400 μg/ml G418 (Geneticin; Gibco-BRL, Gaithersburg, MD, USA).

Western blotting analysis- To analyze TrkB signaling, wild type and mutant huntingtin striatal cells were placed in DMEM serum-free medium for 3 h and then exposed to BDNF (100 ng/ml), EGF (25 ng/ml) or PMA (1 μM) for different time periods (0, 5, 15 and 30 min). To analyze the neuroprotective role of ERK1/2 activation against oxidative stress, wild type and mutant huntingtin striatal cells were treated with 200 μM H_2O_2 or pre-treated with BDNF (100 ng/ml for 15 min) or BDNF in the presence of the MEK inhibitor PD98059 (10 μM, for 15 min) before H_2O_2 treatment. Total cellular extracts were collected in lysis buffer containing 50 mM Tris base (pH 7.4), 150 mM NaCl, 2 mM EDTA, 0.1 mM phenylmethylsulphonyl fluoride, 1 % NP-40, and supplemented with 1 mM sodium orthovanadate and protease inhibitor cocktail (Sigma-Aldrich). Samples were centrifuged at 10,000 x *g* for 10 min and the protein contents determined by (Detergent-Compatible) Protein Assay (Bio-Rad; Hercules, CA, USA). Protein extracts (30 μg) were mixed with 5 x SDS sample buffer, boiled for 5 min, resolved by 6-10 % SDS–polyacrylamide gel electrophoresis and transferred to nitrocellulose membranes (Schleicher & Schuell; Keene, NH, USA). Blots were blocked in 10 % non-fat powdered milk in TBS-T (50 mM Tris-HCl, 150 mM NaCl, pH 7.4, 0.05 % Tween 20) for 30 min at room temperature. The membranes were then incubated overnight at 4°C with primary antibodies (Phospho p44/42 ERK1/2 (1/1000), total ERK1/2 (1/2500), Phospho-MEK1/2 (Ser217/221) (1/1000), total MEK1/2 (1/1000), Phospho-c-Raf (Ser338) (1/1000), total c-Raf (1/1000), Phospho-Akt (Ser473) (1/1000), total Akt (1/1000),

Phospho-PLC-γ (Tyr783) (1/1000), PLC-γ (1/1000), phospho-Trk (Tyr 496/490) (1/1000), total TrkB (1/500), total Shc (1/1000), total IRS-1 (1/1000), total Ras (1/2500), anti-HA (1/1000) or α-tubulin (1:50,000)). The membranes were then rinsed three times with TBS-T and incubated with horseradish peroxidase-conjugated secondary antibody for 1 h at room temperature. After washing for 30 min with TBS-T, the membranes were developed using the enhanced chemiluminescence substrate kit (Santa Cruz Biotechnology). The Gel-Pro densitometry program (Gel-Pro Analyzer for Windows- version 4.0.00.001) was used to quantify the different immunoreactive bands relative to the intensity of the α-tubulin band in the same membranes. Data are expressed as the mean ± SD of band density obtained in three independent experiments.

Surface biotinylation and Western blot analysis of TrkB- Surface TrkB receptors were measured by biotinylation followed by Western blot using a specific antibody that only recognizes full-length TrkB isoforms (Santa Cruz Biotechnology, Santa Cruz, CA, USA), as described elsewhere (16). Wild type and mutant huntingtin striatal cells were incubated in Sulfo-NHS-LC Biotin (0.5 mg/ml; Pierce Chemical, Rockford, IL, USA) in cold PBS with Ca^{2+} and Mg^{2+}, for 30 min. The surface biotinylation was stopped by removing the above solution and incubating the cells in 10 mM ice-cold glycine in PBS for 20 min. Cells were washed three times with cold PBS with Ca^{2+} and Mg^{2+} and additional once with cold PBS and then harvested and lysed in lysis buffer containing 50 mM Tris base (pH 7.4), 150 mM NaCl, 2 mM EDTA, 0.1 mM phenylmethylsulphonyl fluoride, 1 % NP-40, and supplemented with 1 mM sodium orthovanadate and protease inhibitor cocktail (Sigma-Aldrich). Samples were centrifuged at 10,000 x *g* for 10 min and the protein contents determined by (Detergent-Compatible) Protein Assay (Bio-Rad; Hercules, CA, USA). Surface biotinylated TrkB receptors were immunoprecipitated from total extracts (500 µg) by Immunopure Immobilized Streptavidine (Pierce Chemical), separated by 6 % SDS-PAGE and subjected to Western blot using a polyclonal anti-TrkB antibody (Santa Cruz).

Immunocytochemistry and fluorescence microscopy analysis- Wild type and mutant huntingtin striatal cells were plated at a density of 6 x 10^5/well (triplicate wells), fixed in 4 % (w/w) paraformaldehyde for 15 min to detect surface TrkB immunostaining or fixed and then permeabilized in PBS containing 0.1 % saponin (5 min) to visualize total TrkB and Ras protein. Blocking was done in 1 % bovine serum albumin (BSA) in PBS for 1 h and cells were then incubated for 2 h in blocking solution containing anti TrkB antibody (extracellular domain, 1/100, Millipore), anti-TrkB (total TrkB, 1/500, Santa Cruz) or anti-Ras antibody (1/200, BD Bioscience). After several washes in PBS (3 x 5 min), cells were then incubated for 1 h in blocking solution containing Cy2-conjugated anti-mouse (1:200) or Cy3-conjugated anti-rabbit (1:300) (Invitrogen, Carlsbad, CA). For TrkB staining, cells were examined by confocal microscopy using a TCS SL laser scanning confocal spectral microscope (Leica Microsystems Heidelberg, Mannheim, Germany) with argon and HeNe lasers attached to a DMIRE2 inverted microscope (Leica Microsystems Heidelberg). Images were taken using a 63x numerical aperture objective with a 4x digital zoom and standard (1 Airy disk) pinhole. For each cell, the entire three-dimensional stack of images from the ventral surface to the top of the cell was obtained by using the Z drive in the TCS SL microscope. For Ras staining cells were observed with a BX60 epifluorescence microscope (Olympus, Tokyo, Japan) with an Orca-ER cooled CCD camera (Hamamatsu Photonics, Japan). TrkB and Ras immunofluorescence was quantified using the ImageJ version 1.33 by Wayne Rasband (National Institutes of Health). In all cases, 20-25 cells were randomly selected from at least three independent cultures.

To analyze the sensitivity of wild type and mutant huntingtin striatal cells to oxidative stress, striatal cells were treated for 30 min in DMEM medium containing 200 µM H_2O_2. Cells were then fixed in 4 % formaldehyde in PBS for 15 min, washed in PBS (3 × 5min) and permeabilized for 10 min with PBS containing 0.1 % saponin and 1 % bovine serum albumin. Actin cytoskeleton was visualized by incubating cells for 30 min with 0.1 mg/ml of TRITC-labeled phalloidin. Stained cells were observed with a BX60

epifluorescence microscope (Olympus, Tokyo, Japan) with an Orca-ER cooled CCD camera (Hamamatsu Photonics, Japan).
To analyze whether PMA-neuroprotection from H_2O_2 involved PKC activation, MAPK signaling was inhibited in wild type and mutant huntingtin striatal cells by incubation with the MEK inhibitor PD098059 (10μM for 15 min) prior to PMA treatment (1μM for 15 min) and H_2O_2-induced cell death was determined by analysis of actin cytoskeleton.

Cell survival- Cell survival was quantified by counting the total number of cells in treated conditions versus vehicle-treated conditions (100 %). Forty fields were counted per condition and experiment, comprising at least 20-25 cells. Data are given as mean ± SD of values obtained in three independent experiments performed in triplicate.

Ras activation assay- Wild type and mutant huntingtin striatal cells were stimulated with BDNF (100 ng/ml) or EGF (25 ng/ml) for 15 min, harvested with the lysis buffer (the same as that for Western blot) and cleared by centrifugation at 10,000 x *g* for 10 min at 4ºC. Aliquots of lysates were set aside to allow quantification of total Ras by immunoblotting. Equal amounts of the remainder lysates were incubated for 90 min at 4ºC with beads coated with fusion protein (GST-Raf1-RBD) consisting of GST fused to the Ras binding domain of Raf-1 (Millipore). Beads were washed three times with cold PBS containing 0.1 % NP-40 and additional once with cold PBS. Bound protein was eluted for 5 min with 5 X Laemmli sample buffer at 95ºC and analyzed by immunoblotting for Ras.

Cell Transfection- For the study of Ras-dependent induction of ERK1/2 pathway wild-type and mutant huntingtin striatal cells were transfected using Lipofectamine 2000 as described by the manufacturer (Invitrogen, CA, USA). Wild type and mutant huntingtin cells at 70 % confluence were transfected with HA-RasV12, a constitutively active form of Ras (generously provided by Dr N. Agell, University of Barcelona, Spain) and the protein extracts were prepared 24 h post-transfection.

Luciferase assay- The luciferase vector pGL3 Basic vector containing the promoter 2 (P2) of the trkB gene (1600trkBP2-Luc) (17) was kindly provided by Dr Rodriguez-Peña (CSIC-UAM, Madrid, Spain). Briefly, wild type and mutant huntingtin striatal cells were seeded into 24-well plates and co-transfected (Lipofectamine 2000, Invitrogene) with P2-CRE-TrkB-Luc (0.3 μg) and the pRL-TK construct (0.25 μg) (Promega, Wisconsin, USA), which produces Renilla luciferase as a control for transfection efficiency. At 24 h after transfection, cells were lysed with Glo Lysis buffer, and firefly and Renilla luciferase activities in cell lysates were sequentially measured using the Dual-Luciferase Reported Assay System (Promega) and luminometer (BIO-TEK Clarity). Firefly luciferase luminescence was normalized by Renilla luciferase luminescence. The mean values for each construct were obtained from three independent experiments performed in triplicate.
Quantitative (Q)-PCR assays- Total RNA from wild type and mutant huntingtin striatal cells was extracted using the Total RNA Isolation Nucleospin® RNA II Kit (Macherey-Nagel, Düren, Germany). Total RNA (500 ng) was used to synthesize cDNA using random primers with the StrataScript® First Strand cDNA Synthesis System (Stratagene, La Jolla, CA, USA). The cDNA synthesis was performed at 42 °C for 60 min in a final volume of 20 μl according to manufacturer's instructions. The cDNA was then analyzed by Q-PCR using the following TaqMan® Gene Expression Assays (Applied Biosystems, Foster City, CA, USA): 18S (Hs99999901_s1) and p52/p46 Shc (Mm00468940_m1). Reverse-transcriptase (RT)-polymerase chain reaction (PCR) was performed in 25 μl volumes on 96-well plates, in a reaction buffer containing 12.5 μl Brilliant® Q-PCR Master Mix (Stratagene), 1.25 μl TaqMan® Gene Expression Assays, and 1 ng of cDNA. Reactions included 40 cycles of a two-step PCR; 95 ºC for 30 sec and 60 ºC for 1 min, after initial denaturation at 95 °C for 10 min. All Q-PCR assays were performed in duplicate and repeated for at least three independent experiments. To provide negative controls and exclude contamination by genomic DNA, the RT was omitted in the cDNA synthesis step, and the samples were subjected to the PCR reaction

in the same manner with each TaqMan® Gene Expression Assay. The Q-PCR data were analyzed using the MxPro™ Q-PCR analysis software version 3.0 (Stratagene). Quantification was performed with the Comparative Quantitation Analysis program of the mentioned software and using the 18S gene expression as internal loading control.

Statistical analysis- All the data were analyzed with the program Graph Pad Prism version 4.0 (GraphPad Software; San Diego, CA, USA). Results are expressed as mean ± SD. Experimental data was analyzed by Student's *t*-test. A value of $p \leq 0.05$ was accepted as denoting statistical significance.

RESULTS

Mutant STHdh^{Q111} striatal cells express reduced levels of cell-surface TrkB receptors- Decreased mRNA and protein levels of TrkB receptors; have previously been described by our group in several HD models (11). Given the importance of cell-surface TrkB receptors for activation of BDNF signaling, we first investigated by biotinylation and Western blotting the expression of cell-surface TrkB in immortalized wild type STHdh^{Q7} and mutant STHdh^{Q111} striatal cells. These cells express endogenous levels of normal and mutant huntingtin with 7 and 111 glutamines, respectively and provide an accurate genetic HD cell model (15). In agreement with our previous results (11) we found a significant reduction (48 % ± 15 %, $p \leq 0.01$) of total TrkB levels in mutant huntingtin striatal cells compared to wild type cells (Fig. 1A). Notably, surface TrkB levels were reduced by 35 % ± 10 % ($p \leq 0.05$) in the biotinylated fraction of mutant huntingtin cells compared to wild type cells whereas no differences were found on total and cell-membrane EGFR levels.

We next examined whether reduced TrkB expression was associated with transcriptional deficits. Given that the *trkB* gene is a target of CREB transcription (18) and altered CREB/CBP pathway has previously been shown in mutant STHdh^{Q111} striatal cells (9), we have analyzed CRE-TrkB transcriptional activity in wild type and mutant huntingtin striatal cells by luciferase reporter gene assay. As shown in Fig. 1B, a significant decrease of CRE-TrkB luciferase activity was detected in mutant compared to wild type striatal cells, suggesting that TrkB transcriptional deregulation may be involved in reduced TrkB expression in mutant huntingtin striatal cells.

To further analyze the expression and distribution of cell-surface TrkB receptors, immunocytochemistry analysis was performed in permeable (Fig. 2A) and non-permeable (Fig. 2B) wild type and mutant huntingtin striatal cells. According to the biochemical data, a significant reduction of total TrkB staining was revealed in mutant compared to wild type cells (40 % ± 10 %; $p \leq 0.001$). Notably, when cell-surface TrkB expression was examined using an antibody against the extracellular domain of TrkB in non-permeable wild type and mutant huntingtin striatal cells, a punctuate TrkB staining that was significantly lower in mutant compare to wild type cells was revealed (29 % ± 7 %; $p \leq 0.001$). Moreover, whereas a homogenous distribution of TrkB was observed in mutant cells, enriched-TrkB membrane patches were detected in wild type cells (Fig. 2B). Altogether, these results indicate that mutant huntingtin leads to a specific reduction and altered distribution of cell-surface TrkB receptors in striatal cells.

Specific reduction of TrkB-mediated ERK1/2 activation in mutant STHdh^{Q111} striatal cells- TrkB-mediated signaling involves the activation of the Ras/MAPK/ERK1/2, PI3K/Akt and PLC-γ pathways (12-14;19). To determine whether BDNF-induced TrkB signaling was also affected by mutant huntingtin expression, we evaluated BDNF-mediated ERK1/2, Akt and PLC-γ activation in wild type STHdh^{Q7} and mutant STHdh^{Q111} huntingtin striatal cells. Cells were treated with BDNF for 0-30 min, and total cell extracts were collected and analyzed by Western blot using specific antibodies. BDNF treatment induced a similar increase of Akt (Ser473) and PLC-γ (Tyr783) phosphorylation in both wild type and mutant huntingtin striatal cells (Fig. 3A and 3B, respectively), which suggest that both Akt and PLC-γ signaling are properly activated even in the presence of lower TrkB receptors in mutant huntingtin cells. In contrast to Akt and PLC-γ, BDNF-mediated activation of MAPK/ERK1/2 pathway was significantly

reduced in mutant compared to wild type cells. Thus, while in wild type cells BDNF treatment caused a robust and time-dependent activation of MAPK signaling detected as increased phosphorylation of ERK1/2, MEK and c-Raf, in mutant huntingtin striatal cells BDNF failed to increase phosphorylation of ERK1/2, MEK and c-Raf (Fig. 3C).

We next examined whether impaired BDNF-mediated ERK1/2 activation was specific for TrkB or a general mechanism associated with activation of growth factor receptors. Wild type and mutant huntingtin striatal cells were treated with EGF and the levels of p-ERK1/2 were evaluated by Western blot analysis (Fig. 3D). Importantly, mutant huntingtin striatal cells exhibited similar time-dependent EGF-induced ERK1/2 phosphorylation than wild-type striatal cells. These findings demonstrate that mutant huntingtin interferes specifically with BDNF TrkB-mediated ERK 1/2 signaling in striatal cells.

TrkB phosphorylation is not altered in mutant STHdh^{Q111} striatal cells- The activation of BDNF-mediated TrkB signaling depends on TrkB phosphorylation (12-14;19). To test whether reduced TrkB phosphorylation might explain the lack of BDNF-mediated ERK1/2 activation observed in mutant huntingtin striatal cells, we next analyzed the levels of phospho-Tyr490 TrkB, the Tyr residue critical for activation of Ras/MAPK/ERK1/2 and PI3K/Akt pathways. Western blot and quantitative analysis demonstrated similar time-dependent TrkB phosphorylation induced by BDNF in wild type and mutant huntingtin striatal cells (Fig. 4). These findings suggest that mutant huntingtin does not impair BDNF-induced TrkB signaling by altering TrkB phosphorylation and activation.

Mutant huntingtin interferes with BDNF signaling at the level of docking proteins- Phosphorylation of TrkB at Tyr-490 provides critical binding sites to adapter proteins such Shc and IRS involved on TrkB activation of Ras/MAPKs and PI3K/Akt, respectively (12;19;20). We then tested the hypothesis that mutant huntingtin could interfere with BDNF-ERK1/2 mediated activation by altering the levels of particular TrkB adapter proteins. Western blot analysis revealed that levels of the p52/p46 Shc isoforms were significantly reduced in mutant cells compared to those of wild type cells (30 % ± 13%, $p \leq 0.001$). By contrast, p66 Shc levels, which are not involved on Ras activation (21) and IRS-1 that participates on PI3/Akt activation (12;22), were similar in both genotypes (Fig. 5A).

To determine whether the reduction in p52/p46 Shc protein levels resulted from reduced mRNA expression, quantitative-PCR analysis of total mRNA derived from wild type and mutant huntingtin striatal cells was performed (Fig. 5B). Q-PCR analysis revealed a significant decrease (40 % ± 6 %, $p \leq 0.01$) in p52/p46 Shc mRNA in mutant huntingtin compared to wild type striatal cells, which suggest that altered p52/p46 Shc transcription is involved in diminished p52/p46 Shc protein expression. All together, these results support the idea that impaired BDNF-mediated ERK1/2 activation caused by mutant huntingtin may involve the specific reduction of the adapter proteins p52/p46 Shc.

BDNF-mediated Ras activation is impaired in mutant STHdh^{Q111} striatal cells- Activation of Ras by neurotrophic factors promotes neuronal cell survival and differentiation (12-14;20). Following BDNF stimulation, the adaptor proteins p52/p46 Shc are recruited to phosphorylated Tyr-490 on TrkB receptors ensuing transient activation of Ras protein (14;20). Therefore, we examined whether decreased expression of Shc proteins in mutant huntingtin striatal cells attenuates ERK1/2 signaling by altering Ras activation. We first determined total Ras expression in cell extracts obtained from wild type and mutant huntingtin striatal cells. As shown in Fig. 6A the levels of Ras in wild type cells were similar than those in mutant cells. According to these biochemical data, immunocytochemistry analysis demonstrated similar levels and distribution of Ras in wild type and mutant huntingtin striatal cells (Fig. 6A).

We then determined Ras activation induced by BDNF stimulation by measuring the levels of Ras-GTP (23). Active Ras-GTP was pulled-down with a GST fusion protein containing the Ras binding domain of Raf-1 (GST-Raf1-RBS) and blotted with a Ras antibody. Ras activity measured in BDNF-treated wild-type cell was increased by 7-fold

compared to untreated wild type cells, whereas BDNF-induced Ras activation was undetectable in mutant huntingtin cells (Fig. 6B). By contrast, EGF induced Ras activation was comparable between wild type and mutant huntingtin striatal cells (17 and 14 fold-increase, respectively, Fig. 6B). Taken together these results demonstrate that defective Ras activation is involved on altered BDNF-induced ERK1/2 activation in mutant huntingtin striatal cells.

Finally, to further evaluate the contribution of altered Ras activation on impaired BDNF-mediated ERK1/2 activation, wild type and mutant huntingtin striatal cells were transfected with a constitutively active HA-Ras (HA-RasV12) and levels of phosphorylated ERK1/2 were detected by Western blot analysis (Fig. 6C). Expression of Ras-V12 in mutant cells restored ERK1/2 phosphorylation to levels of wild type cells. These results indicate that defective Ras activation rather than down-stream components of the TrkB pathway (Raf, MEK or ERK1/2) underlies altered MAPK activation in mutant huntingtin striatal cells.

ERK1/2 activation is required for protection of mutant STHdh^{Q111} striatal cells against oxidative stress- The Ras/ERK1/2 pathway is a critical signaling cascade mediating neuroprotection against oxidative stress-induced cell death (21;24-28). To investigate the consequences of reduced ERK1/2 activation on the neuroprotective response to oxidative stress, wild type and mutant huntingtin striatal cells were exposed to H_2O_2 in the presence or absence of BDNF. Oxidative damage was determined by analysis of cell morphology changes on actin cytoskeleton as a measure of cell injury. Untreated wild type cells showed a well-organized actin cytoskeleton (Fig. 7A, panel i) whereas treatment with H_2O_2 induced changes on the actin cytoskeleton detected as rearranged actin stress fibers and a significant reduction of cell survival (Fig. 7A, panel iii). Notably, BDNF treatment completely prevented H_2O_2-induced actin cytoskeleton alterations and cell death (Fig. 7A, panel v). Consistent with a neuroprotective role of ERK1/2 activation against oxidative damage, a significant increase of ERK1/2 phosphorylation was detected in BDNF-treated wild type cells compared to untreated or H_2O_2-treated wild type cells (Fig. 7B, 5-fold and 2-fold respectively, *$p \leq 0.05$)*. By contrast, mutant huntingtin striatal cells exhibited greater sensitivity to identical doses of H_2O_2 than wild type cells demonstrated by reduced cell survival and a higher proportion of cells with altered actin cytoskeleton (Fig. 7A, panel ii and iv). Importantly, BDNF treatment did not protect mutant huntingtin cells from oxidative stress induced by H_2O_2 (Fig. 7A, panel vi). Accordingly, the phosphorylation of ERK1/2 following BDNF incubation was no significantly different from those detected in basal or H_2O_2-treated mutant huntingtin cells (Fig. 7B).

To further confirm the possible role of ERK1/2 activation in the neuroprotection by BDNF, wild type striatal cells were pre-incubated with PD098059 to pharmacologically inhibit MEK, the upstream kinase of ERK1/2. In the presence of the MEK inhibitor, the neuroprotective effect of BDNF against H_2O_2-evoked cell death was completely abrogated (Fig. 7A, panel vii). Control experiments revealed that PD098059 completely inhibited BDNF-induced ERK1/2 phosphorylation in wild type cells (Fig. 7C). Altogether, these results suggest that the higher sensitivity of mutant huntingtin striatal cells to oxidative stress may be related to deficient activation of the ERK1/2 signaling pathway.

Phorbol esters rescue MAPK signaling and protect mutant STHdh^{Q111} striatal cells from oxidative stress- The diacylglycerol analogue phorbol 12-myristate 13-acetate (PMA) may activate Ras independently of the canonical Shc/Grb2/Sos pathway (29). We took advantage of this specific PMA action to investigate whether pharmacological manipulation of the MAPK pathway could rescue mutant huntingtin striatal cells from cell death induced by oxidative stress. As shown in Fig. 8A, PMA treatment induced similar activation of ERK1/2 monitored as levels of ERK1/2 phosphorylation in either wild type or mutant huntingtin striatal cells (Fig. 8A). In addition, PMA increased MEK and Raf phosphorylation with a similar kinetic of activation in wild type and mutant huntingtin striatal cells (Fig. 8A). These results indicate that activation of the MAPK cascade downstream of Shc/Grb2/Sos pathway is not

compromised in mutant huntingtin striatal cells.

We next investigated whether the recovery of MAPK signaling by PMA was able to protect mutant huntingtin striatal cells against oxidative stress induced by H_2O_2. Wild type and mutant cells were incubated with PMA prior to H_2O_2 treatment and cell death was detected by analysis of the actin cytoskeleton pattern. As previously shown (Fig. 7A), mutant huntingtin striatal cells exhibited increased sensitivity to oxidative stress detected by higher number of cells displaying an abnormal actin cytoskeleton pattern. Notably, PMA treatment prevented H_2O_2-induced toxicity either in wild type or mutant huntingtin striatal cells (Fig. 8B).

Given that PMA is a well-known activator of PKC, we then examined whether PMA-neuroprotection from H_2O_2 involved PKC activation. Wild type and mutant huntingtin striatal cells were exposed to PD098059 prior to PMA treatment and H_2O_2-induced cell death was determined by analysis of actin cytoskeleton. Pre-treatment of wild type cells with the MEK inhibitor PD098059 prior to H_2O_2 exposure induced higher cell death compared to those cells only treated with H_2O_2 (Fig. 8B panel v and Fig. 8C panel v) that agrees with our biochemical data showing activation of the ERK1/2 pathway in wild type cells following H_2O_2 treatment (Fig. 7B). Notably, PMA-mediated neuroprotection from H_2O_2-induced toxicity was prevented by exposure of wild type and mutant huntingtin striatal cells to PD098059 (Fig. 8C panel vii and panel viii), which is consistent with a specific role of ERK1/2 activation in the PMA neuroprotective effect.

Taken together, these findings support the view that deficient BDNF-induced ERK1/2 activation underlies the lack of protection against oxidative damage in mutant huntingtin striatal cells.

DISCUSSION

Accumulating evidence suggest that altered neurotrophic support plays a critical role in the neurodegenerative process associated with HD. Reduced BDNF expression and transport have been proposed as the main mechanisms contributing to neurotrophic deficiency in HD (1;4;5;8-10;30). In addition, we have previously demonstrated a significant reduction of the specific BDNF receptor TrkB in HD cellular and mouse models and in HD human brain (11). Based on these previous observations it is important to elucidate whether diminished TrkB expression may involve changes in BDNF-mediated signaling and neuroprotection. In this study we have shown reduced levels of total and cell-surface TrkB receptors as a result of mutant huntingtin expression. Notably, reduced TrkB expression was associated with decreased CRE-TrkB promoter activity, which suggest that diminished CREB-mediated transcription may account for altered TrkB expression in mutant huntingtin striatal cells

Moreover our results have shown that mutant huntingtin expression has differential effects on BDNF signaling. Thus, while BDNF-mediated Ras/MAPK/ERK1/2 activation was significantly attenuated in mutant compared to wild type cells, no differences were detected in the PI3K/Akt and PLC-γ pathways. This result together with the unchanged phosphorylated levels of TrkB in mutant huntingtin striatal cells, suggest that reduced cell-surface TrkB receptors in mutant cells cannot entirely account for the lack of ERK1/2 activation induced by BDNF treatment. Consistent with this idea, we found in mutant huntingtin striatal cells a specific reduction at the level of mRNA and protein of p52/46Shc, the scaffolding proteins that couple the activated TrkB receptors to Ras/MAPK/ERK1/2 pathway (12-14;20). Importantly, p66Shc that is not involved in ERK1/2 activation was unaffected. Similar to p66Shc expression, the levels of IRS-1, a well known adaptor protein involved in BDNF-mediated PI3K/Akt activation (12;14;22) were unchanged. These findings together with the fact that BDNF may also activates the PI3K/Akt pathway by direct association of PI3K with the phosphorylated form of TrkB receptors and that PLC-γ is also directly activated by binding to phospho-TrkB (12-14) may explain the selective disruption of the Ras/MAPK/ERK1/2 signaling in mutant huntingtin striatal cells. Notably, our studies revealed that in striatal cells mutant huntingtin impairs TrkB-induced ERK1/2 activation without affecting EGFR-mediated MAPK signaling, even though ERK1/2 by EGFR also involves activation of p52/46 Shc proteins. Recruitment of Shc adapter proteins

to tyrosine receptors is a key event to the subsequent interaction with Grb2/Sos complexes and the activation of the Ras-MAPK signaling pathway (20;32). The specific mechanisms underlying recruitment of Shc proteins to tyrosine receptors remains poorly characterized. It has been suggested that the efficiency of tyrosine kinase receptors to recruit Shc proteins may be dependent on the Shc residues and/or domains phosphorylated by these receptors (20;33-35). Thus, while insulin receptors can efficiently phosphorylate p52Shc but not p46Shc, EGFR leads to efficient phosphorylation and recruitment of both isoforms (20;36). In addition, the phosphorylation of Shc at different residues/domains is also critical to recruit Grb2/Sos complexes to the membrane, which facilitates Ras/MAPK activation (20;32-35;37). Therefore a possible scenario will be those in which mutant huntingtin specifically disrupts TrkB-mediated ERK1/2 signaling by (1) reducing levels of Shc adapter proteins and (2) by preferentially interfering with the recruitment and phosphorylation of Shc/Grb2/Sos complexes to TrkB receptors. In agreement with this view it has been reported that association of Grb2 to TrkA receptors following NGF stimulation was disrupted by over-expressing full length mutant huntingtin (38). Consistent with impaired coupling of TrkB to Shc complexes, we found reduced Ras activation following BDNF treatment in mutant huntingtin striatal cells. Moreover, over-expression of HA-RasV12, a constitutively active form of Ras, or PMA treatment, that directly activates c-Raf, restored MAPK signaling in mutant huntingtin striatal cells. These results support the idea that mutant huntingtin disrupts ERK1/2-mediated TrkB signaling upstream of Ras activation.

Our findings demonstrating diminished BDNF-mediated ERK1/2 activation in mutant huntingtin striatal cells raise the question whether lack of TrkB-dependent ERK1/2 signaling might contribute to HD pathology. Multiple evidences have implicated oxidative stress linked to mitochondrial dysfunction in HD neuropathology (39;40). Accumulation of oxidative markers ranging from DNA strand breaks, protein nitration or lipid oxidative damage have been demonstrated in several HD mouse models as in HD brain (39-42). Notably, ERK1/2 activation plays an important neuroprotective role mediating cell survival in response to oxidative stress (24-28). Therefore, we hypothesized that reduced BDNF-induced ERK1/2 activation could result in increased susceptibility of mutant huntingtin striatal cells to oxidative injury. We found that cell viability was significantly decreased in mutant huntingtin striatal cells compared to wild type cells when exposed to H_2O_2. Importantly, pre-treatment with BDNF protected wild type but not mutant huntingtin striatal cells against oxidative stress. Indeed, the protective effect of BDNF was blocked by treatment with the MEK1/2 inhibitor PD 098059. Together these results demonstrate that the protective effect of BDNF against oxidative damage in striatal cells is mediated by activation of ERK1/2 and that activation of ERK1/2 in striatal cells is critical to mediate neuroprotection against oxidative stress. Accordingly, pharmacological activation of the MAPK pathway with PMA prevents cell death induced by oxidative stress in mutant huntingtin striatal cells. Consistent with a protective role of ERK1/2 in HD, it has been reported that activation of ERK1/2 protects against mutant huntingtin-associated toxicity in PC12 cells and in immortalized striatal neuronal cells that express exon-1 mutant huntingtin (43;44). Moreover, orthovanadate treatment, a tyrosine phosphatase inhibitor that reduces the dephosphorylation of ERK1/2, decreases caspase-3 activation and cell death in PC12 cells expressing full-length mutant huntingtin (44).

In summary, our studies have identified the reduction in p52/p46Shc adapter protein expression as the principal mechanism by which mutant huntingtin selectively impairs TrkB-mediated ERK1/2 activation. We propose that by reducing the expression of p52/p46Shc adapter proteins, mutant huntingtin might disturbs the formation of TrkB-Shc signaling complexes resulting in decreased Ras-mediated activation and decreased MAPK activation. We found that such inhibition increases mutant huntingtin striatal cell vulnerability to oxidative stress suggesting that the lack of ERK1/2 activation might contribute to HD neurodegeneration.

Altogether our data strongly support the view that pharmacological strategies targeting BDNF but also targeting selectively MAPK/ERK1/2 pathway might provide better

benefits to HD treatment that those only aimed to raise BDNF levels.

REFERENCE LIST

1. Canals, J. M., Pineda, J. R., Torres-Peraza, J. F., Bosch, M., Martin-Ibanez, R., Munoz, M. T., Mengod, G., Ernfors, P., and Alberch, J. (2004) *J.Neurosci.* **24,** 7727-7739

2. Fumagalli, F., Molteni, R., Calabrese, F., Maj, P. F., Racagni, G., and Riva, M. A. (2008) *CNS.Drugs* **22,** 1005-1019

3. Perez-Navarro, E., Canudas, A. M., Akerund, P., Alberch, J., and Arenas, E. (2000) *J.Neurochem.* **75,** 2190-2199

4. Zuccato, C. and Cattaneo, E. (2007) *Prog.Neurobiol.* **81,** 294-330

5. Zuccato, C., Ciammola, A., Rigamonti, D., Leavitt, B. R., Goffredo, D., Conti, L., MacDonald, M. E., Friedlander, R. M., Silani, V., Hayden, M. R., Timmusk, T., Sipione, S., and Cattaneo, E. (2001) *Science* **293,** 493-498

6. Zuccato, C., Tartari, M., Crotti, A., Goffredo, D., Valenza, M., Conti, L., Cataudella, T., Leavitt, B. R., Hayden, M. R., Timmusk, T., Rigamonti, D., and Cattaneo, E. (2003) *Nat.Genet.* **35,** 76-83

7. Duan, W., Guo, Z., Jiang, H., Ware, M., Li, X. J., and Mattson, M. P. (2003) *Proc.Natl.Acad.Sci.U.S.A* **100,** 2911-2916

8. Ferrer, I., Goutan, E., Marin, C., Rey, M. J., and Ribalta, T. (2000) *Brain Res.* **866,** 257-261

9. Gines, S., Seong, I. S., Fossale, E., Ivanova, E., Trettel, F., Gusella, J. F., Wheeler, V. C., Persichetti, F., and MacDonald, M. E. (2003) *Hum.Mol.Genet.* **12,** 497-508

10. Zuccato, C., Marullo, M., Conforti, P., MacDonald, M. E., Tartari, M., and Cattaneo, E. (2008) *Brain Pathol.* **18,** 225-238

11. Gines, S., Bosch, M., Marco, S., Gavalda, N., Diaz-Hernandez, M., Lucas, J. J., Canals, J. M., and Alberch, J. (2006) *Eur.J.Neurosci.* **23,** 649-658

12. Kaplan, D. R. and Miller, F. D. (2000) *Curr.Opin.Neurobiol.* **10,** 381-391

13. Patapoutian, A. and Reichardt, L. F. (2001) *Curr.Opin.Neurobiol.* **11,** 272-280

14. Reichardt, L. F. (2006) *Philos.Trans.R.Soc.Lond B Biol.Sci.* **361,** 1545-1564

15. Trettel, F., Rigamonti, D., Hilditch-Maguire, P., Wheeler, V. C., Sharp, A. H., Persichetti, F., Cattaneo, E., and MacDonald, M. E. (2000) *Hum.Mol.Genet.* **9,** 2799-2809

16. Du, J., Feng, L., Yang, F., and Lu, B. (2000) *J.Cell Biol.* **150,** 1423-1434

17. Barettino, D., Pombo, P. M., Espliguero, G., and Rodriguez-Pena, A. (1999) *Biochim.Biophys.Acta* **1446,** 24-34

18. Deogracias, R., Espliguero, G., Iglesias, T., and Rodriguez-Pena, A. (2004) *Mol.Cell Neurosci.* **26,** 470-480

19. Skaper, S. D. (2008) *CNS.Neurol.Disord.Drug Targets.* **7,** 46-62

20. Ravichandran, K. S. (2001) *Oncogene* **20,** 6322-6330 Ref ID: 39

21. Arany, I., Faisal, A., Nagamine, Y., and Safirstein, R. L. (2008) *J.Biol.Chem.* **283,** 6110-6117

22. Yamada, M., Ohnishi, H., Sano, S., Nakatani, A., Ikeuchi, T., and Hatanaka, H. (1997) *J.Biol.Chem.* **272,** 30334-30339

23. Reynolds, L. F., de Bettignies, C., Norton, T., Beeser, A., Chernoff, J., and Tybulewicz, V. L. (2004) *J.Biol.Chem.* **279,** 18239-18246

24. Cavanaugh, J. E., Jaumotte, J. D., Lakoski, J. M., and Zigmond, M. J. (2006) *J.Neurosci.Res.* **84,** 1367-1375

25. Gu, L., Cui, T., Fan, C., Zhao, H., Zhao, C., Lu, L., and Yang, H. (2009) *Biochem.Biophys.Res.Commun.* **383,** 469-4741

26. Han, B. H. and Holtzman, D. M. (2000) *J.Neurosci.* **20,** 5775-5781

27. Huang, H. Y., Lin, S. Z., Kuo, J. S., Chen, W. F., and Wang, M. J. (2007) *Neurobiol.Aging* **28,** 1258-1269

28. Jiang, H., Zhang, L., Koubi, D., Kuo, J., Groc, L., Rodriguez, A. I., Hunter, T. J., Tang, S., Lazarovici, P., Gautam, S. C., and Levine, R. A. (2005) *J.Mol.Neurosci.* **25,** 133-140

29. Rubio, I., Rennert, K., Wittig, U., Beer, K., Durst, M., Stang, S. L., Stone, J., and Wetzker, R. (2006) *Biochem.J.* **398,** 243-256

30. Gauthier, L. R., Charrin, B. C., Borrell-Pages, M., Dompierre, J. P., Rangone, H., Cordelieres, F. P., De Mey, J., MacDonald, M. E., Lessmann, V., Humbert, S., and Saudou, F. (2004) *Cell* **118,** 127-138

31. Ventura, A., Luzi, L., Pacini, S., Baldari, C. T., and Pelicci, P. G. (2002) *J.Biol.Chem.* **277,** 22370-22376

32. Luzi, L., Confalonieri, S., Di Fiore, P. P., and Pelicci, P. G. (2000) *Curr.Opin.Genet.Dev.* **10,** 668-674

33. Gotoh, N., Muroya, K., Hattori, S., Nakamura, S., Chida, K., and Shibuya, M. (1995) *Oncogene* **11,** 2525-2533

34. Gotoh, N., Tojo, A., and Shibuya, M. (1996) *EMBO J.* **15,** 6197-6204

35. Gotoh, N., Toyoda, M., and Shibuya, M. (1997) *Mol.Cell Biol.* **17,** 1824-1831

36. Okada, S., Yamauchi, K., and Pessin, J. E. (1995) *J.Biol.Chem.* **270,** 20737-20741

37. Velazquez, L., Gish, G. D., van Der, G. P., Taylor, L., Shulman, J., and Pawson, T. (2000) *Blood* **96,** 132-138

38. Liu, Y. F., Deth, R. C., and Devys, D. (1997) *J.Biol.Chem.* **272,** 8121-8124

39. Browne, S. E. and Beal, M. F. (2006) *Antioxid.Redox.Signal.* **8,** 2061-2073

40. Butterworth, N. J., Williams, L., Bullock, J. Y., Love, D. R., Faull, R. L., and Dragunow, M. (1998) *Neuroscience* **87,** 49-53

41. Polidori, M. C., Mecocci, P., Browne, S. E., Senin, U., and Beal, M. F. (1999) *Neurosci.Lett.* **272,** 53-56

42. Stack, E. C., Matson, W. R., and Ferrante, R. J. (2008) *Ann.N.Y.Acad.Sci.* **1147,** 79-92

43. Apostol, B. L., Illes, K., Pallos, J., Bodai, L., Wu, J., Strand, A., Schweitzer, E. S., Olson, J. M., Kazantsev, A., Marsh, J. L., and Thompson, L. M. (2006) *Hum.Mol.Genet.* **15,** 273-285

44. Wu, Z. L., O'Kane, T. M., Scott, R. W., Savage, M. J., and Bozyczko-Coyne, D. (2002) *J.Biol.Chem.* **277,** 44208-44213

FOOTNOTES

Acknowledgements
The authors thank M. Macdonald for providing the huntingtin knock-in striatal cell lines and N.Agell for HA-RasV12. We are very grateful to Cristina Herranz, Ana Lopez and M. Teresa Muñoz for technical assistance. We thank members of our laboratory for helpful discussion. This work was supported by grants from Ministerio de Ciencia e Innovación (SAF2008-00644 to S.G and SAF2008-04360 to J.A), Centro de Investigaciones Biomédicas en Red sobre Enfermedades Neurodegenerativas (CIBERNED CB06/05/0054), Fondo de Investigaciones Sanitarias (Instituto de Salud Carlos III, RETICS: RD06/0010/0006 and Fundació La Marató de TV3. P.P is a fellow granted by CIBERNED.

FIGURE LEGENDS

FIGURE 1. **Reduced levels of cell-surface TrkB receptors in STHdh^{Q111} striatal cells.**
A. Representative Western Blot showing the levels of total and cell-surface TrkB and EGFR receptors from wild type (ST7/7Q) and mutant (ST111/111Q) huntingtin striatal cells. Surface TrkB receptors and EGFR were detected by Western blotting after surface protein biotinylation and immunoprecipitation of biotinylated proteins by streptavidine-agarose beads. Total TrkB and EGFR were determined by Western blot of whole cell lysates. The histogram represents the percentage of TrkB expression relative to wild type values. Values are given as mean ± SD of three independent experiments. **p≤0.01, *p≤0.05 as determined by Student's *t*-test.
B. Histogram showing the transcription activity of the P2-CRE-TrkB promoter in transiently transfected wild type (ST7/7Q) and mutant huntingtin (ST111/111Q) striatal cells. The histogram represents the percentage of luciferase activity relative to wild type values. Values are given as mean ± SD of three independent experiments. ***p≤0.001 as determined by Student's *t*-test.

FIGURE 2. **Altered cell-surface TrkB distribution in STHdh^{Q111} striatal cells.**
Overlay of confocal and corresponding differential interference contrast (DIC) images of TrkB immunofluorescence in permeabilized (A) and non-permeabilized (B) wild type (ST7/7Q) and mutant (ST111/111Q) huntingtin striatal cells. TrkB distribution is showed in a pseudo-color scale. Warm colors represent maximum intensities, whereas cold colors are representative of low intensities (the intensity of each pixel was set to 255 levels of grey). Images represent the projection of the two slices containing the maximal cross-section of the cell nucleus. Confocal images show reduced total (A) and cell-surface (B) TrkB immunoreactivity in mutant huntingtin

striatal cells (ST111/111Q). Histograms represent the mean of the TrkB fluorescence intensity ± SD of three independent experiments. ***p≤0.001. Bar scale 10μm.

FIGURE 3. **Specific inhibition of BDNF-induced MAPK signaling in STHdh^{Q111} striatal cells.** Representative Western Blots showing the time course of BDNF-induced phosphorylation of Akt (***A***) and PLC-γ (***B***) in wild-type (ST7/7Q) and mutant (ST111/111Q) huntingtin striatal cells. Whole cell lysates were blotted with antibodies against phosphorylated Ser473 Akt (p-Akt), total Akt, phosphorylated Tyr783 (p-PLC-γ), total PLC-γ and α-tubulin as a loading control, after stimulating with 100 ng/ml BDNF for the indicated time periods. The results are representative of three independent experiments. ***C.*** Representative Western Blot showing the time course of BDNF-induced phosphorylation of MAPK signaling proteins in wild-type (ST7/7Q) and mutant (ST111/111Q) huntingtin striatal cells. Whole cell lysates were blotted with antibodies against phosphorylated ERK1/2 (p-ERK1/2), MEK (p-MEK) and cRaf (p-cRaf) as well as total ERK1/2, MEK and c-Raf and α-tubulin as a loading control, after stimulating with 100 ng/ml BDNF for the indicated time periods. The histograms represent the relative p-ERK/ERK, p-MEK/MEK and p-Raf/Raf ratios expressed as percentage versus control cells. Values are given as mean ± SD of three independent experiments. ***p≤0.001 as determined by Student's *t*-test. ***D.*** Representative Western Blot showing the time course of EGF-induced phosphorylation of ERK1/2 in wild-type (ST7/7Q) and mutant (ST111/111Q) huntingtin striatal cells. Whole cell lysates were blotted with antibodies against phosphorylated ERK1/2 (p-ERK1/2) and total ERK1/2 after stimulating with 25 ng/ml EGF for the indicated time periods. The results are representative of three independent experiments.

FIGURE 4. **Mutant huntingtin does not interfere with BDNF-induced TrkB phosphorylation in STHdh^{Q111} striatal cells.** Representative Western Blot showing levels of Tyr-490 phosphorylated TrkB (p-TrkB), total TrkB (TrkB) and α-tubulin as a loading control from wild-type (ST7/7Q) and mutant (ST111/111Q) cell extracts obtained after treatment with 100 ng/ml BDNF for the indicated time periods. The histogram represents the percentage of TrkB induction (p-TrkB/TrkB) relative to control wild type or mutant striatal cells. Values are given as mean ± SD of three independent experiments. ***p≤0.001, $^{+}$p≤0.05, $^{+++}$p≤0.001 as determined by Student's *t*-test.

FIGURE 5. **Specific reduction of protein adaptors p52/46 Shc in STHdh^{Q111} striatal cells.** ***A***. Representative Western Blot showing levels of p52/46 Shc, p66 Shc and IRS-1 and α-tubulin as a loading control in total cell extracts obtained from wild-type (ST7/7Q) and mutant (ST111/111Q) huntingtin striatal cells. The histograms represent the percentage of p52/46 Shc, p66 Shc and IRS-1 expression relative to wild type values. Values are given as mean ± SD of three independent experiments. ***p≤0.001 as determined by Student's *t*-test. ***B.*** Quantitative-PCR analysis of p52/46 Shc mRNA levels. The histogram represents the relative p52/46 Shc mRNA levels expressed as percentage versus wild type cells. Values are given as mean ± SD of three independent experiments performed in duplicate. **p≤0.01 as determined by Student's *t*-test.

FIGURE 6. **BDNF-induced Ras activation is impaired in STHdh^{Q111} striatal cells.** ***A.*** *(upper panel)* Representative Western blot showing levels of Ras and α-tubulin as a loading control in total cell extracts obtained from wild-type (ST7/7Q) and mutant (ST111/111Q) huntingtin striatal cells. The results are representative of three independent experiments. *(lower panel)* Representative immunofluorescence images showing similar expression and distribution of Ras protein in wild-type (ST7/7Q) and mutant (ST111/111Q) huntingtin striatal cells. Bar scale 10 μm. Histogram represents the mean of the Ras fluorescence intensity expressed as percentage versus wild type cells. Values are given as mean ± SD of three independent experiments. ***B***. Representative Western blot showing levels of GTP-loaded Ras. Activated (GTP-bound) Ras pool was detected by immunoblotting of pull-down experiments from total cell lysates of untreated and BDNF or EGF treated wild type and mutant huntingtin striatal

cells. Aliquots of the total cell extracts were analyzed in parallel to ascertain equal loading. The results are representative of three independent experiments. ***C***. Representative Western blot showing levels of p-ERK1/2, ERK1/2 and α-tubulin as a loading control in total cell extracts from wild type (ST7/7Q) and mutant (ST111/111Q) huntingtin striatal cells. Whole cells extracts were obtained from wild type and mutant huntingtin cells treated with BDNF (100 ng/ml 15 min) or transfected with a constitutively active form of Ras (HA-RasV12) and blotted with antibodies against phosphorylated ERK1/2 (p-ERK1/2), total ERK1/2 (ERK1/2), HA and α-tubulin as a loading control. The results are representative of four independent experiments.

FIGURE 7. **ERK1/2 activation is required for BDNF-mediated neuroprotection against oxidative stress in STHdh^{Q111} striatal cells.**
A. Representative immunofluorescence images showing rodamine-phalloidin staining to visualize the actin cytoskeleton in wild-type (ST7/7Q) and mutant (ST111/111Q) huntingtin striatal cells. Wild-type and mutant huntingtin striatal cells were exposed to H_2O_2 (200 μM for 15 min) in the absence (panels iii and iv) or presence of 100 ng/ml BDNF (panels v and vi) and cell viability was detected by actin cytoskeleton patterning. The inhibition of the neuroprotective effect of BDNF in the presence of the MEK inhibitor PD098059 is shown in Panel (vii). The pre-incubation period with BDNF provides protection against oxidative injury in wild type but not mutant huntingtin striatal cells. Notice the higher number of H_2O_2 treated mutant cells with altered cytoskeleton rearrangements compared to wild type cells (Panel iv and vi, arrows). The results are representative of three independent experiments. Bar scale 10μm. Histograms represent the percentage of cell survival relative to control cells. ***p≤0.001 as determined by Student's *t*-test. ***B.*** Wild-type (ST7/7Q) and mutant (ST111/111Q) huntingtin striatal cells were exposed to H_2O_2 (200 μM for 30 min) in the absence or presence of BDNF (100 ng/ml for 15 min) and total extracts were analyzed by Western blot, using antibodies against phosphorylated ERK1/2 (p-ERK1/2), total ERK1/2 (ERK1/2) or α- tubulin as a loading control. An example of Western blot is presented. The results are representative of three independent experiments. ***C.*** Wild type (ST7/7Q) striatal cells were treated with BDNF (100 ng/m, 15 min) in the absence or presence of the MEK inhibitor PD098059 (10μM, 15 min). The cells were then challenged with H_2O_2 (200 μM, 30 min) and total extracts were analyzed by Western blot, using antibodies against phosphorylated ERK1/2 (p-ERK1/2), total ERK1/2 (ERK1/2) or α- tubulin as a loading control. An example of Western blot is presented. The results are representative of three independent experiments.

FIGURE 8**. PMA treatment restores ERK1/2 activation and prevents cell injury induced by oxidative stress in STHdh^{Q111} striatal cells.** ***A.*** Representative Western Blot showing the time course of PMA-induced phosphorylation of MAPK signaling proteins in wild-type (ST7/7Q) and mutant (ST111/111Q) huntingtin striatal cells. Whole cell lysates were blotted with antibodies against phosphorylated ERK1/2 (p-ERK1/2), MEK (p-MEK) and cRaf (p-cRaf) as well as total ERK1/2, MEK and c-Raf and α-tubulin as a loading control, after stimulating with PMA for the indicated time periods. The results are representative of three independent experiments. ***B***. Representative immunofluorescence images showing rodamine-phalloidin staining to visualize the actin cytoskeleton in wild-type (ST7/7Q) and mutant (ST111/111Q) huntingtin striatal cells. Wild-type (ST7/7Q) and mutant (ST111/111Q) huntingtin striatal cells were exposed to H_2O_2 (200 μM, 30 min) in the absence (panels v and vi) or presence of PMA (panels vii and viii) and cell viability was detected by actin cytoskeleton patterning. The pre-incubation with PMA provides protection against oxidative injury in both wild type and mutant huntingtin striatal cells. ***C***. Representative immunofluorescence images showing rodamine-phalloidin staining to visualize the actin cytoskeleton in wild-type (ST7/7Q) and mutant (ST111/111Q) huntingtin striatal cells. MAPK signaling was inhibited in wild type (ST7/7Q) and mutant (ST111/111Q) huntingtin striatal cells by incubation with the MEK inhibitor PD098059 prior to PMA treatment and H_2O_2-induced cell death was determined by analysis of actin cytoskeleton. The pre-incubation with PD98059 prevents PMA-mediated protection against oxidative injury in both wild type and mutant huntingtin striatal cells (panel vii and viii, arrows). The results are representative of three independent experiments. Bar scale 10μm.

FIGURE 9. **Proposed role of mutant huntingtin in reducing TrkB-mediated ERK1/2 activation in striatal cells**. BDNF-TrkB activation involves ERK1/2 activation by recruitment of Shc/Grb2/Sos complexes to phosphorylated TrkB receptor (wild type cells). Mutant huntingtin disrupts BDNF-mediated induction of MAPK signaling by reducing expression of p52/46 Shc adapter proteins and interfering with TrkB-Shc mediated Ras activation. Reduced BDNF-mediated ERK1/2 activation in mutant huntingtin striatal cells leads to increased cell vulnerability to oxidative stress. This model is supported first by the ability of PD098059 to prevent BDNF-mediated neuroprotection in wild type cells and second by the capacity of PMA, that may activate Ras independently of Shc/Grb2/Sos complexes, to protect mutant huntingtin cells against oxidative damage.

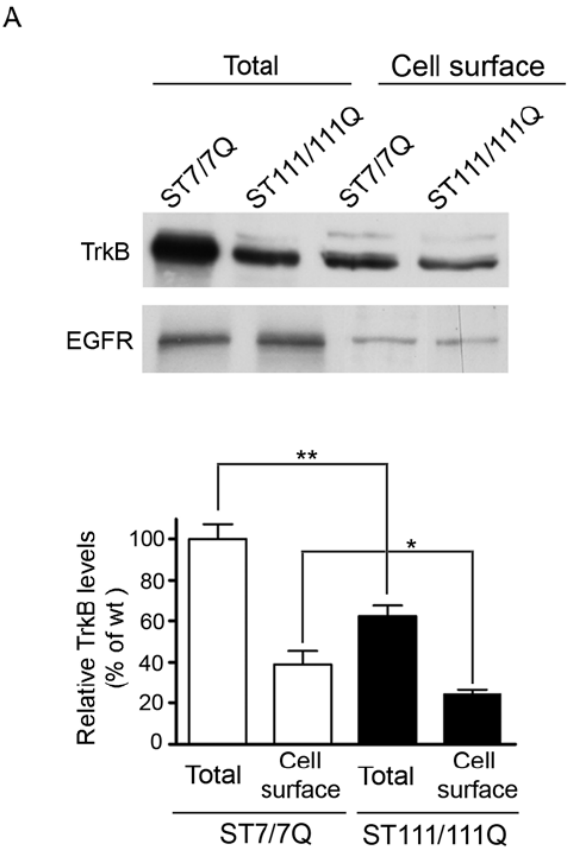
A
Total
Cell surface
ST7/7Q
ST111/111Q
ST7/7Q
ST111/111Q
TrkB
EGFR
**
*
Relative TrkB levels
(% of wt)
100
80
60
40
20
0
Total
Cell surface
Total
Cell surface
ST7/7Q
ST111/111Q

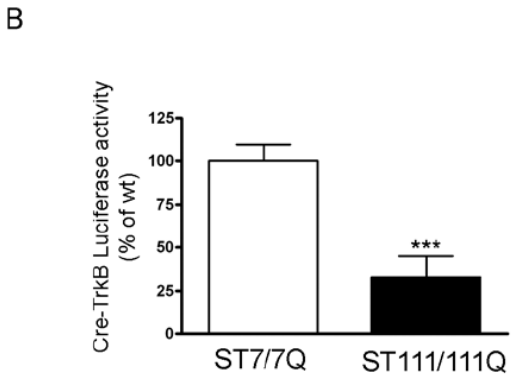
B
Cre-TrkB Luciferase activity
(% of wt)
125
100
75
50
25
0
***
ST7/7Q
ST111/111Q

Figure 1

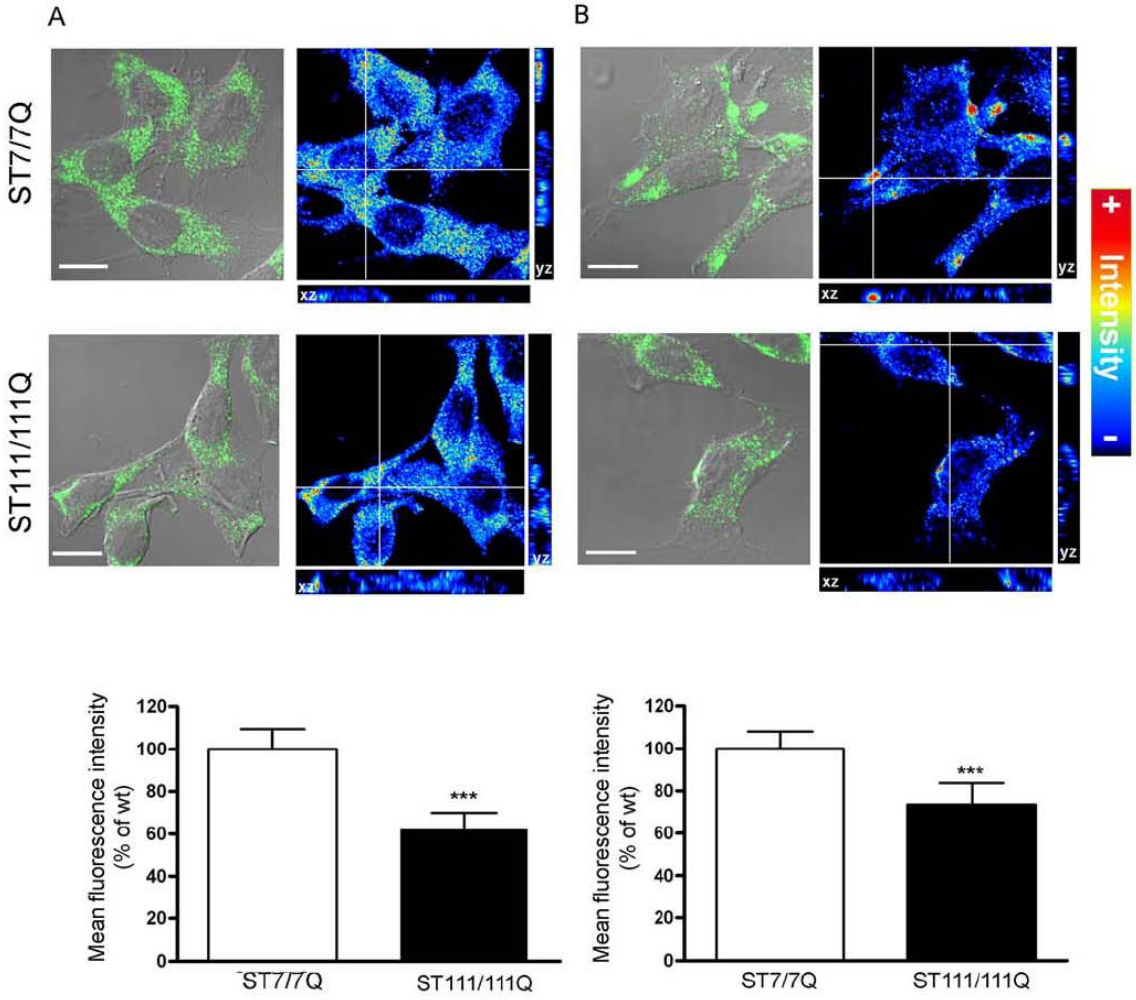
A
B
ST7/7Q
ST111/111Q
xz
yz
+
Intensity
-
Mean fluorescence intensity (% of wt)
120
100
80
60
40
20
0
***
ST7/7Q
ST111/111Q

Figure 2

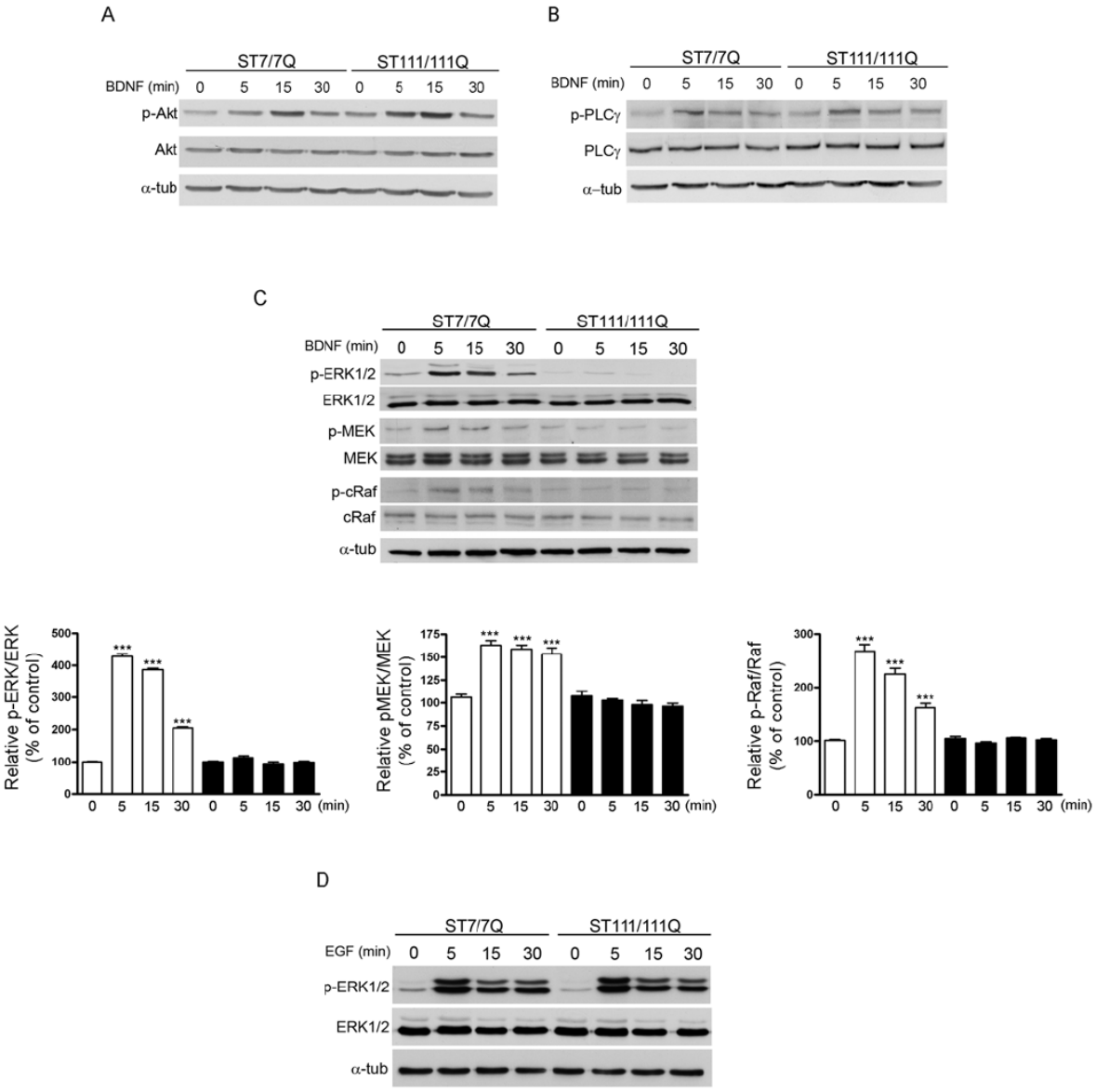
A
ST7/7Q
ST111/111Q
BDNF (min) 0 5 15 30 0 5 15 30
p-Akt
Akt
α-tub
B
ST7/7Q
ST111/111Q
BDNF (min) 0 5 15 30 0 5 15 30
p-PLCγ
PLCγ
α–tub
C
ST7/7Q
ST111/111Q
BDNF (min) 0 5 15 30 0 5 15 30
p-ERK1/2
ERK1/2
p-MEK
MEK
p-cRaf
cRaf
α-tub
Relative p-ERK/ERK (% of control)
Relative pMEK/MEK (% of control)
Relative p-Raf/Raf (% of control)
0 5 15 30 0 5 15 30 (min)
***
D
ST7/7Q
ST111/111Q
EGF (min) 0 5 15 30 0 5 15 30
p-ERK1/2
ERK1/2
α-tub

Figure 3

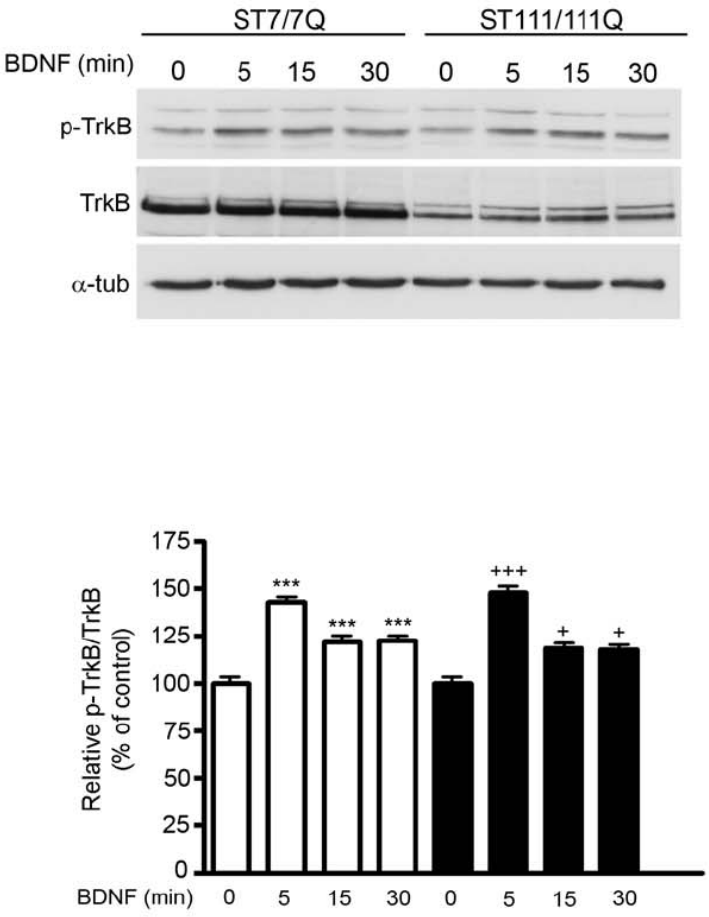
ST7/7Q
ST111/111Q
BDNF (min)
0
5
15
30
0
5
15
30
p-TrkB
TrkB
α-tub
Relative p-TrkB/TrkB (% of control)
175
150
125
100
75
50
25
0
***
***
***
+++
+
+
BDNF (min)
0
5
15
30
0
5
15
30

Figure 4

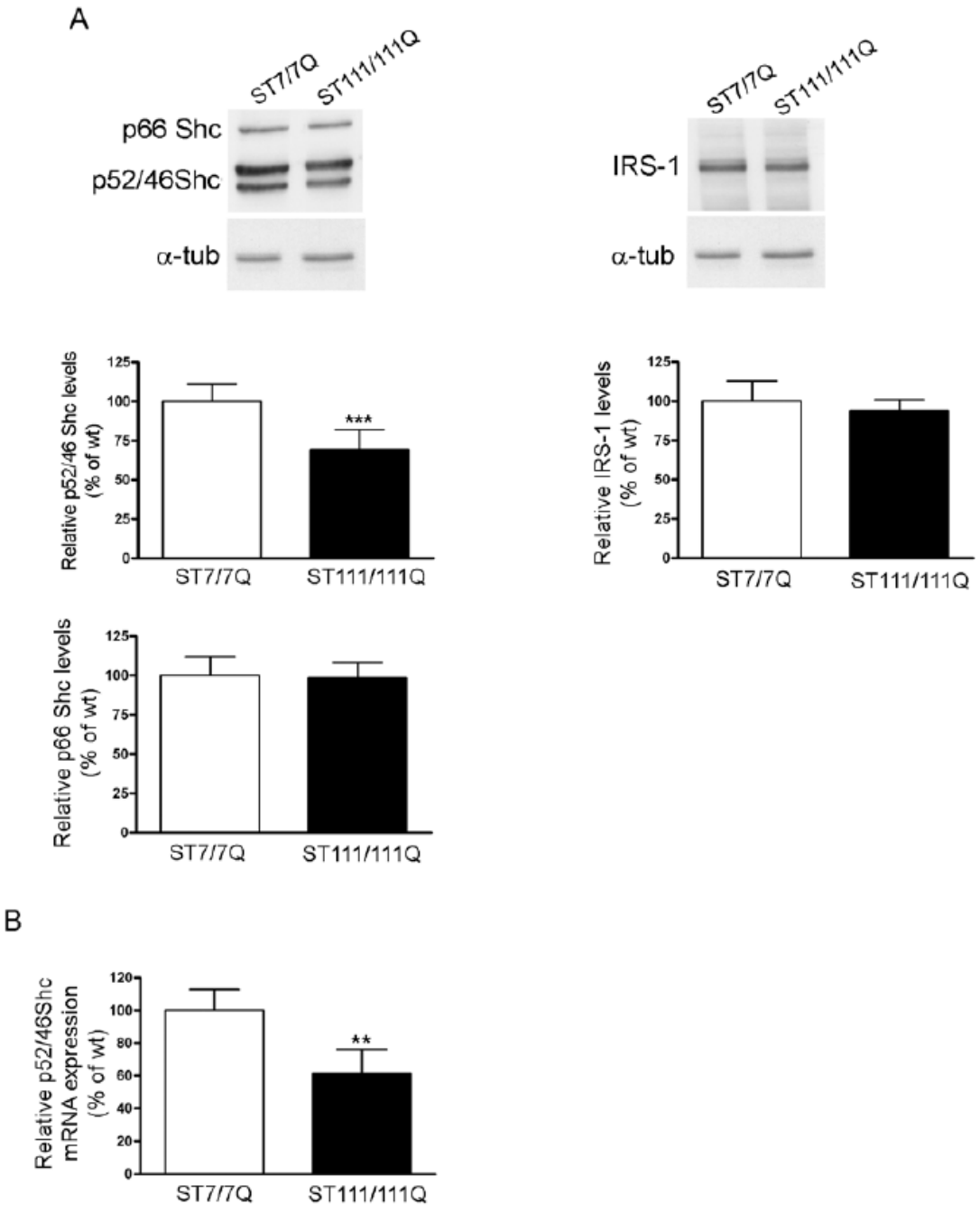
A
ST7/7Q
ST111/111Q
p66 Shc
p52/46Shc
α-tub
IRS-1
Relative p52/46 Shc levels (% of wt)
Relative IRS-1 levels (% of wt)
Relative p66 Shc levels (% of wt)
***
B
Relative p52/46Shc mRNA expression (% of wt)
**

Figure 5

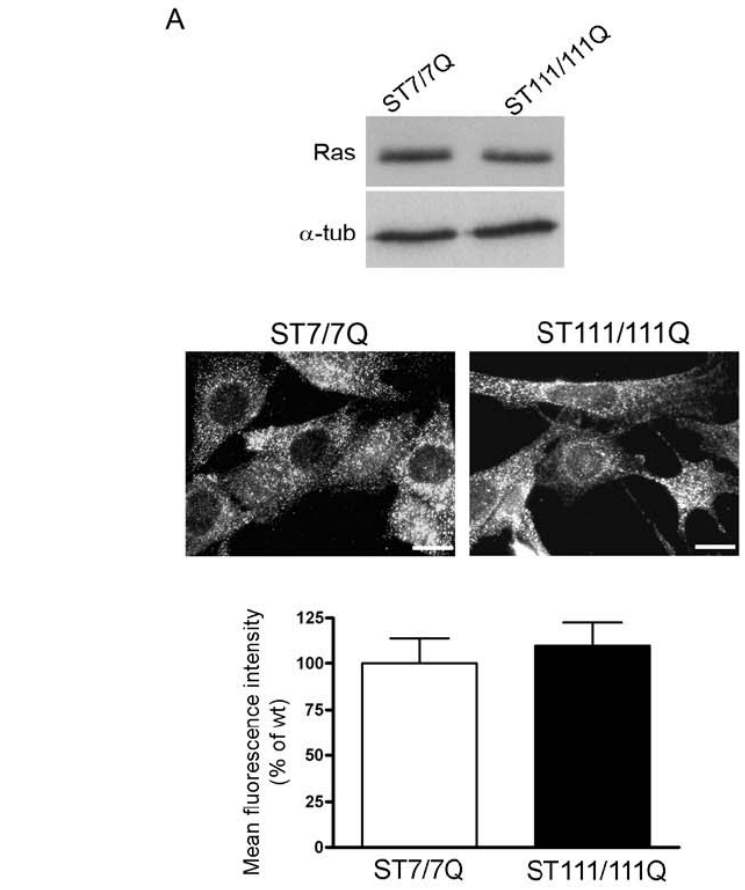
A
ST7/7Q
ST111/111Q
Ras
α-tub
ST7/7Q
ST111/111Q
Mean fluorescence intensity (% of wt)
125
100
75
50
25
0
ST7/7Q
ST111/111Q
B
ST7/7Q
ST111/111Q
Ras-GTP pulldown
IB: anti-Ras
CNT BDNF EGF CNT BDNF EGF
Total cell lysates
IB: anti-Ras
C
ST7/7Q
ST111/111Q
CNT BDNF Ras V12 CNT BDNF Ras V12
p-ERK1/2
ERK1/2
HA
α-Tub

Figure 6

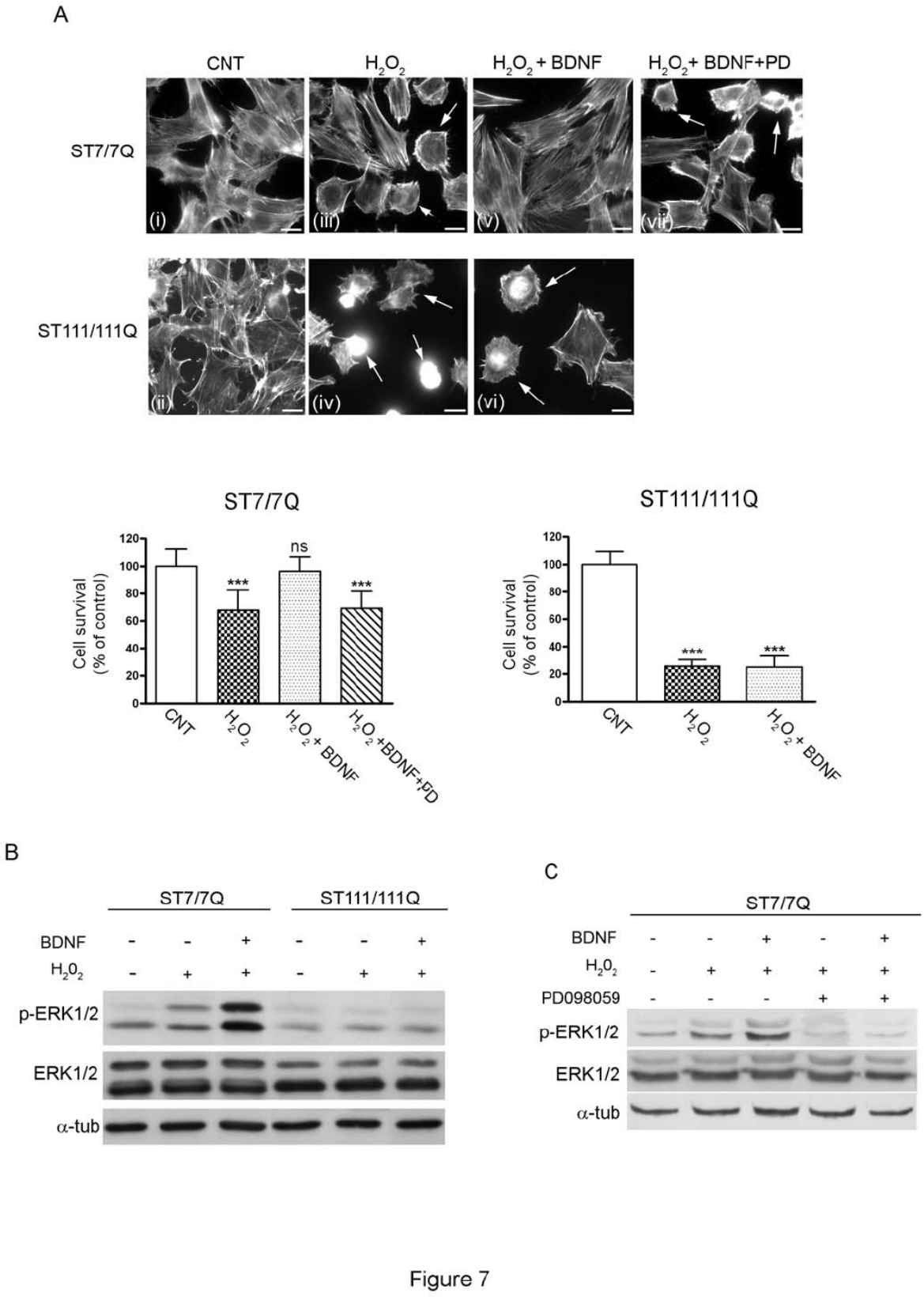
A
CNT
H2O2
H2O2 + BDNF
H2O2+ BDNF+PD
ST7/7Q
ST111/111Q
(i)
(iii)
(v)
(vii)
(ii)
(iv)
(vi)
ST7/7Q
Cell survival (% of control)
ns
***
***
CNT
H2O2
H2O2 + BDNF
H2O2 +BDNF+PD
ST111/111Q
Cell survival (% of control)
***
***
CNT
H2O2
H2O2 + BDNF
B
ST7/7Q
ST111/111Q
BDNF
H2O2
p-ERK1/2
ERK1/2
α-tub
C
ST7/7Q
BDNF
H2O2
PD098059
p-ERK1/2
ERK1/2
α-tub

Figure 7

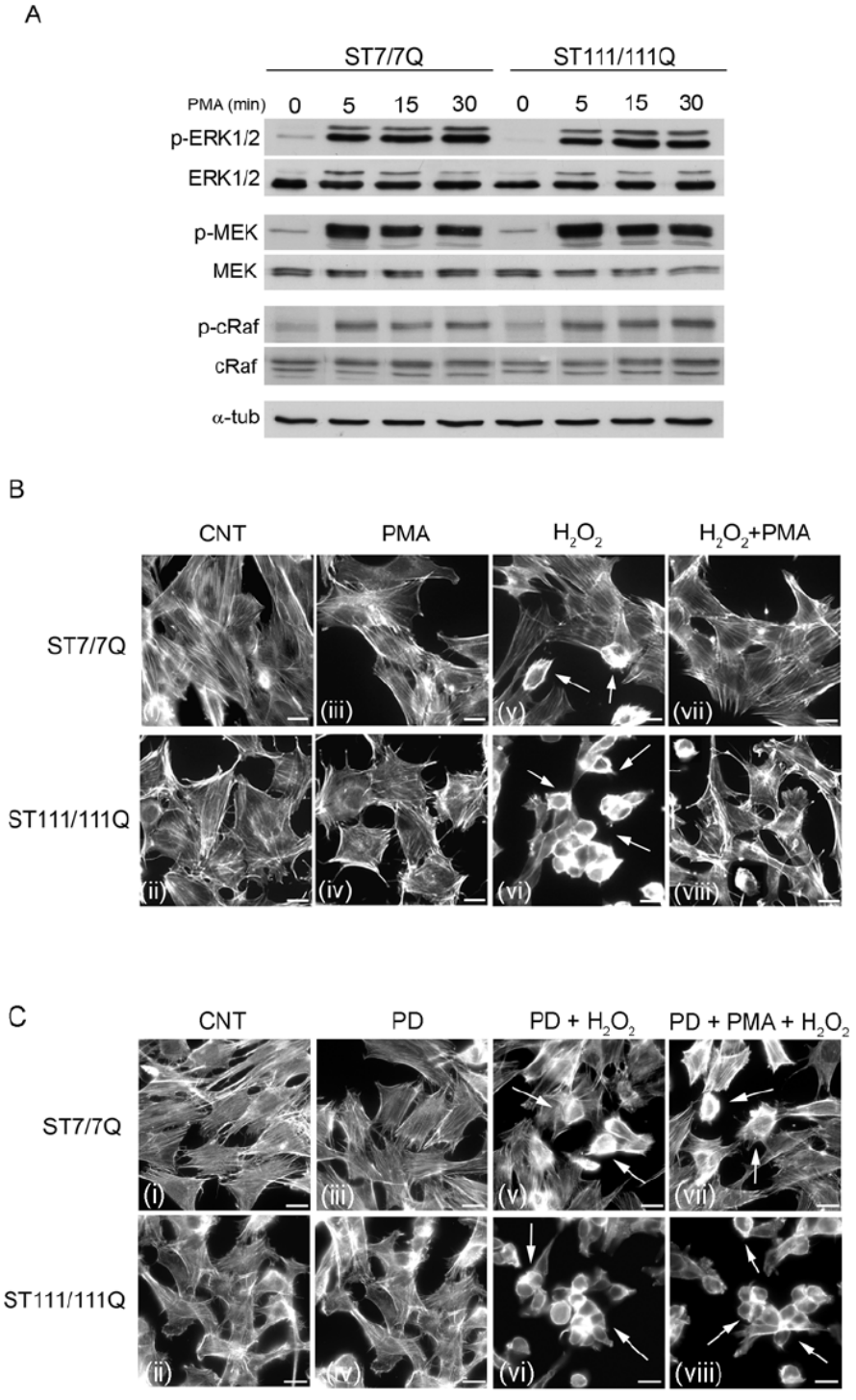
A
ST7/7Q
ST111/111Q
PMA (min) 0 5 15 30 0 5 15 30
p-ERK1/2
ERK1/2
p-MEK
MEK
p-cRaf
cRaf
α-tub
B
CNT
PMA
H2O2
H2O2+PMA
ST7/7Q
ST111/111Q
(i)
(ii)
(iii)
(iv)
(v)
(vi)
(vii)
(viii)
C
CNT
PD
PD + H2O2
PD + PMA + H2O2
ST7/7Q
ST111/111Q
(i)
(ii)
(iii)
(iv)
(v)
(vi)
(vii)
(viii)

Figure 8

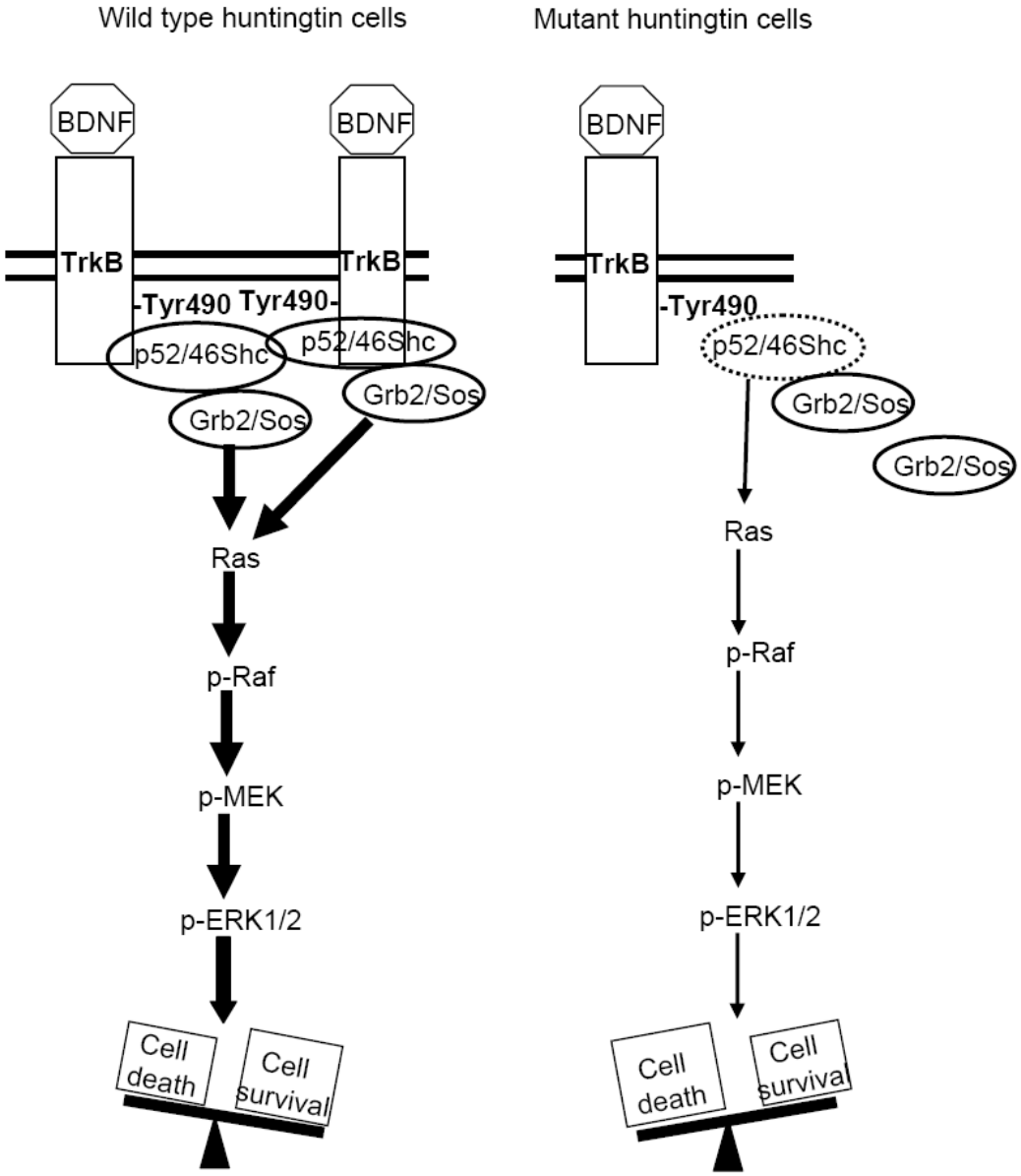
Wild type huntingtin cells
Mutant huntingtin cells
BDNF
BDNF
BDNF
TrkB
TrkB
TrkB
-Tyr490 Tyr490-
-Tyr490
p52/46Shc
p52/46Shc
p52/46Shc
Grb2/Sos
Grb2/Sos
Grb2/Sos
Grb2/Sos
Ras
Ras
p-Raf
p-Raf
p-MEK
p-MEK
p-ERK1/2
p-ERK1/2
Cell death
Cell survival
Cell death
Cell survival

Figure 9